Published in final edited form as:

Acta Biomater. 2022 February ; 139: 118–140. doi:10.1016/j.actbio.2021.08.031.

Electroconductive biomaterials for cardiac tissue engineering⋆

Hamid Esmaeili[a], **Alejandra Patino-Guerrero**[a], **Masoud Hasany**[b], **Mohammad Omaish Ansari**[c], **Adnan Memic**[c], **Alireza Dolatshahi-Pirouz**[d,e], **Mehdi Nikkhah**[a,f,1,*]

[a]School of Biological and Health Systems Engineering, Arizona State University, Tempe, AZ, USA

[b]Cell Isolation and Transplantation Center, Department of Surgery, Geneva University Hospitals and University of Geneva, Geneva, Switzerland

[c]Center of Nanotechnology, King Abdulaziz University, Jeddah 21589, Saudi Arabia

[d]Department of Health Technology, Technical University of Denmark, 2800 Kgs, Lyngby, Denmark

[e]Department of Health Technology, Technical University of Denmark, Center for Intestinal Absorption and Transport of Biopharmaceuticals, 2800 Kgs, Lyngby, Denmark

[f]Biodesign Virginia G. Piper Center for Personalized Diagnostics, Arizona State University, Tempe, AZ, USA

Abstract

Myocardial infarction (MI) is still the leading cause of mortality worldwide. The success of cell-based therapies and tissue engineering strategies for treatment of injured myocardium have been notably hindered due to the limitations associated with the selection of a proper cell source, lack of engraftment of engineered tissues and biomaterials with the host myocardium, limited vascularity, as well as immaturity of the injected cells. The first-generation approaches in cardiac tissue engineering (cTE) have mainly relied on the use of desired cells (*e.g.*, stem cells) along with non-conductive natural or synthetic biomaterials for *in vitro* construction and maturation of functional cardiac tissues, followed by testing the efficacy of the engineered tissues *in vivo*. However, to better recapitulate the native characteristics and conductivity of the cardiac muscle, recent approaches have utilized electroconductive biomaterials or nanomaterial components within engineered cardiac tissues. This review article will cover the recent advancements in the use of electrically conductive biomaterials in cTE. The specific emphasis will be placed on the use of different types of nanomaterials such as gold nanoparticles (GNPs), silicon-derived nanomaterials, carbon-based nanomaterials (CBNs), as well as electroconductive polymers (ECPs) for engineering of functional and electrically conductive cardiac tissues. We will also cover the recent progress in the use of engineered electroconductive tissues for *in vivo* cardiac regeneration

---

⋆Part of the Special Issue on Conductive and Electroactive Biomaterials and Bio-electronics, guest-edited by Professors Jonathan Rivnay and Mehdi Nikkhah.

*Corresponding author at: School of Biological and Health Systems Engineering, Arizona State University, Tempe, AZ, USA. mnikkhah@asu.edu (M. Nikkhah).

[1]Guest editors did not participate in, or have access to, the peer-review process for manuscripts on which they were an author.

Declaration of Competing Interest

There are no conflicts to declare.

applications. We will discuss the opportunities and challenges of each approach and provide our perspectives on potential avenues for enhanced cTE.

Keywords

Cardiac tissue engineering; Myocardial infarction; Gold nanoparticles; Carbon-based nanomaterials; Electroconductive polymers; Injectable conductive biomaterials

1. Introduction

Heart failure (HF) is the number one cause of morbidity worldwide [1]. Although HF could be treated with pharmacological administration or implantation of left ventricular assist devices, heart transplantation still remains the only viable approach for the treatment of HF [2]. However, the clinical success of heart transplantation has been notably hindered due to the scarcity of donor hearts and immune rejection upon transplantation [3]. A single myocardial infarction (MI) can result in the loss of 25% of 2–4 billion cardiomyocytes (CMs) present in the left ventricle (LV) [4]. In contrast to the hearts of lower vertebrates such as adult zebrafish, neonatal mice, and neonatal swine, the adult human heart possesses a significantly limited regenerative capacity with a minimal annual replication rate of CMs (< 1%) [5].

After MI, the LV's healing process is mediated by a programmed cellular response that clears dead cells and matrix debris upon the development of the fibrotic scar tissue [6]. Numerous cell-based as well as cell-free strategies, have been proposed to date to promote regeneration of the injured host tissue upon MI [7]. Examples of cell-based therapies mainly include direct intramyocardial injection of non-CMs such as mesenchymal stem cells (MSCs) [8, 9], cardiac stem cells ($Sca\text{-}1^{+}$ cells) [10, 11], as well as exogenous cells such as human pluripotent stem cell-derived CMs (hPSC-CMs) [12–15], which often result in myocardial repair to some extent. For instance, using a non-human primate MI model, intramyocardially injected human embryonic stem cell-derived CMs (hESC-CMs) into infarcted hearts resulted in remuscularization and electromechanical synchronization [13]. In another study, delivery of the allogenic iPSC-CMs improved cardiac function three months post-transplantation [15]. However, in the majority of these studies, it has been reported that only about 1% of injected cells were grafted at one month post-injection into the host myocardium [16]. Furthermore, ventricular arrhythmias and potential teratoma formation are the other major drawbacks of cell-based strategies through bolus injection of cells [17]. Cell-free techniques include, but are not limited to delivery of microRNA, exosomes [18–20], angiogenic growth factors (.g., VEGFA-B, FGF, PDGF-BB) [21–27], as well as acellular injectable hydrogels [28–32] or patches [33]. However, despite improved cardiac function, reduced fibrosis, and increased vessel density [34, 35] reported in these studies, full regeneration of the injured myocardium has not been reported yet, driving the need for developing new and innovative regenerative medicine-based strategies for the treatment of MI.

The engineering of therapeutic biomaterials has been an appealing strategy to enhance the efficacy of cell-based therapies or growth factor delivery. Numerous studies have shown

that engineered biomaterials can improve retention, survival, and engraftment issues often seen with growth factors delivery or cell therapies [36–40]. Naturally-derived biomaterials such as fibrin [41–44], collagen [45–51], chitosan (CHI) [52–56], gelatin [57–59], alginate [44, 60–64], hyaluronic acid [65–67], and extracellular matrix (ECM)-derived matrices [32, 41, 68–72], have been widely utilized as scaffolding biomaterials for revascularization and regeneration of ischemic myocardium. Alternatively, commonly used synthetic matrices for treatment of ischemic myocardium include poly(ethylene glycol) (PEG)-based copolymers [22, 25, 26, 73–81], polylactic- co-glycolic acid (PLGA) [22], polycaprolactone (PCL) [74, 82–84], poly(N-isopropyl acrylamide) (PNIPAAm) [24, 27, 85–93], etc.

Electrical conductivity is an inherent characteristic of the myocardium [94]. The conductive system within the heart comprises the internodal pathways, sinoatrial node (SAN), the bundle of Purkinje fibers, and the atrioventricular node (AVN). The action potential initiated in the SAN [95] propagate to the atrial, internodal pathway, and finally to the AVN. The generated action potential propagates to the ventricular myocardium through Purkinje fibers allowing the myocardial cells to experience these signals and contract synchronously [94]. Following MI, the remaining viable CMs are uncoupled and isolated in the non-conductive scar and fibrotic tissue, resulting in ventricular dysfunction and abnormal electrical signaling propagation [96]. However, delivery of non-conductive biomaterials in the form of injectable hydrogels or transplantable cardiac patches may inhibit the propagation of electrical signals across the infarcted myocardium and, preventing the synchronization of contracting CMs within the scar zone [97]. Admittedly, an electroconductive biomaterial may have the potential for mediating electrical signal propagation across the non-conductive fibrotic tissue. To that end, in the past few years, there has been a tremendous effort in the use of electrically conductive biomaterials in the regeneration of injured myocardium, a feature which was rarely considered in initial attempts of cell-based therapies or tissue engineering strategies.

In this review article, we will cover the application of electroconductive materials in the engineering of functional and biomimetic cardiac tissues for the treatment of MI (summarized in Fig. 1). We will cover the use of various types of nanomaterials, such as gold nanoparticles (GNPs), silicon-derived nanomaterials, carbon-based nanomaterials (CBNs) as well as electroconductive polymers (ECPs) in the development of mature and functional cardiac tissues *in vitro*. We will further broaden our discussion and will provide an in-depth *overview* of the *in vivo* use of electroconductive biomaterials and their delivery methods for cardiac repair after MI. Finally, we will discuss new avenues and our perspectives to establish better strategies for improved cardiac tissue engineering (cTE).

2. *In vitro* applications of electroconductive biomaterials for cTE

Tissue engineering has been shown as a promising strategy to recapitulate the topographical, mechanical, and ECM features of the native cardiac microenvironment [98] for regenerative medicine [7] as well as disease modeling applications [99–101]. As one of the key components, the proper design of biomaterials plays a crucial role in engineering functional and mature cardiac tissues [102]. The developed biomaterials for cTE must meet certain design criteria such as substrate stiffness and flexibility [103], biocompatibility [104], and

appropriate pore size allowing cell and nutrient infiltration [105]. These features have been thoroughly reviewed and addressed in design of first-generation biomaterials such as decellularized matrix [106, 107], collagen [108], fibrin [41–44], CHI [52–56], gelatin [57–59], alginate [44, 60–64], etc. for engineering cardiac tissues. However, the poor electrical conductivity of previously reported biomaterials has been one of the major hurdles in achieving proper function in engineered cardiac tissues (ECTs). To make up this drawback, a new generation of electroconductive biomaterials has been explored by incorporation of conductive materials including gold nanoparticles (GNPs), silicon-derived nanomaterials, carbon-based nanomaterials (CBNs), and electroconductive polymers (ECPs). In this section, we will review the leading advances using these electroconductive nanomaterials or biomaterials for *in vitro* cTE applications.

2.1. Gold nanoparticles (GNPs)

Due to biocompatibility features, ease of fabrication process, and unique electrical characteristics, GNPs, including gold nanospheres (GNSs), gold nanorods (GNRs), and gold nanowires (GNWs), have been shown as promising nanomaterials in biomedical-related applications from imaging to diagnostics and notably in tissue engineering and regenerative medicine [109]. The specific emphasis on using GNPs in regenerative medicine has also emerged from their tunable physicochemical properties that could modulate tissue environment by providing cells with the necessary instructional cues for targeted biological responses such as proliferation, migration, and lineage-specific differentiation [110–113]. Numerous studies have demonstrated that the interactions of gold nanomaterials with CMs promote the electrophysiological response of ECTs, similar to the native myocardium (*i.e.*, heart tissue). In this section, we will review the recent advancements in *in vitro* applications of GNPs for cTE applications.

Porous biomaterials have been widely used in cTE [36], but one of their fundamental limitations is that their pore walls restrict cell-cell interaction and delay electrical signal propagation [114]. To address this issue, the pioneering work of Dvir et al. embedded GNWs within pore walls of microporous alginate scaffolds to enhance the matrix's electroconductivity (Fig. 2A) [115]. In an *in vitro* study, neonatal rat left ventricular cardiac cells (NRVCs) (composed of CMs and cardiac fibroblasts (cFBs)) were cultured on the conductive alginate hydrogel. Administration of stagewise electrical stimulation showed improved expression of connexin-43 (Cx-43), cardiac troponin I (cTnI) as well as sarcomeric α-actinin protein expression along with enhanced synchronous contractility of the cardiac tissues.

The slowed ventricular conduction velocity in cardiac arrhythmias has been associated with poor ventricular gap junctions' electrical coupling [116]. You et al. hypothesized that Cx-43 expression in CMs could be enhanced by using electroconductive scaffolds[117]. To that end, GNSs were homogeneously distributed in a tunable hydrogel scaffold synthesized by mixing thiol-2-hydroxyethyl methacrylate (thiol-HEMA) with HEMA at different mass to volume (thiol-HEMA weight/HEMA volume, w/v) ratios to nanoengineer a conductive hydrogel (40% w/v thiol-HEMA/HEMA) with equivalent stiffness to the native myocardium during systole (600–1600 kPa). Neonatal rat left ventricular myocytes (NRVMs) cultured

on the conductive hydrogel showed improved Cx-43 expression with and without electrical stimulation compared with non-conductive scaffolds (0% w/v thiol-HEMA). Despite the promising outcomes, the conductive hydrogels were coated with fibronectin before cell seeding, which may mask the direct contact of cells and the conductive nanomaterials [117].

GNWs and GNRs have also been successfully incorporated in photo crosslinkable gelatin methacrylate (GelMA) for cTE applications [118, 119]. In a pioneer work, the Nikkhah group included GNRs into GelMA hydrogel to fabricate a hybrid and conductive UV-crosslink-able hydrogel (Fig. 2B) [119]. Electroconductivity as well as mechanical characteristics (*i.e.*, stiffness) were significantly improved in the conductive GelMA compared with non-conductive GelMA. Furthermore, *in vitro* biological studies by seeding NRVMs on the nanoengineered hydrogels for seven days demonstrated significant enhanced cell adhesion, retention, and viability. Furthermore, the seeded cells exhibited improved expression of cardiac-specific markers (*i.e.*, cTnI, Cx-43, and sarcomeric α-actinin) along with synchronous beating and enhanced calcium transient as a function of GNRs concentration [119].

One of the critical challenges in cTE is fabricating a biocompatible scaffold without the risk of immune response and host rejection upon transplantation [32]. To address this issue and to better mimic the *in vivo* fibrous structure and architecture of myocardial tissue, Shevach et al. tested the efficacy of depositing a gold layer, with a thickness of 4 and 10 nm, on fibrous decellularized matrices derived from patients' omental tissues (Fig. 2Ca–d) [120]. NRVCs cultured on the conductive substrates for five days demonstrated enhanced expression of sarcomeric α-actinin and Cx-43 along with the formation of aligned and elongated cells (Fig. 2Ce–g). Notably, the engineered conductive tissues deposited with 4 and 10 nm gold layer exhibited stronger contraction force and faster calcium transient than the non-conductive pristine scaffolds. The same group further developed conductive nanocomposite coiled fiber scaffolds by electrospinning poly(ε-caprolactone) polymer (PCL) followed by depositing gold to ensure the anisotropic electrical impulse propagation through the fabricated cardiac tissue [121]. After seven days, NRVCs cultured on non-conductive scaffolds showed rounded morphology with limited cell spreading. In contrast, cells cultured on the conductive scaffolds possessed an aligned and elongated morphology along with actinin striation.

Native heart tissue is organized intricately from macro- to nano-scale [122]. However, the majority of the previous work solely relied on a random mixture of GNPs within the scaffolds (*i.e.*, only nano-scale cues) that lacked the necessary microscale mechanical cues. To address this need and integrated macro- to nano-scale cues within engineered tissues, in a work by Dvir's group, fibrous scaffolds were fabricated through electrospinning PCL-gelatin hybrid solution, followed by incorporating GNSs onto the surface of the scaffolds [123]. Compared with the non-conductive pristine scaffold, NRVCs cultured on the GNS-incorporated scaffolds assembled into highly aligned and elongated cardiac tissues. In another recent study, Navaei et al. generated micro-topographical grooves (50 μm width and depth) on the surface of GelMA-GNR hybrid hydrogels to simultaneously introduce electrical and topographical cues into the engineered tissue (Fig. 2Da–c) [124]. Highly aligned cardiac tissues resembling the *in vivo* cardiac muscle bundle were formed

upon culturing NRVCs on these engineered hydrogels. Enhanced expression of Cx-43 and sarcomeric α-actinin were also evident upon seven days of cell culture (Fig. 2Dd and e).

Cardiac tissues are primarily fabricated or engineered through the use of microfabrication techniques followed by culturing cardiac cells on the surface of the substrates. Although this method is straightforward and accessible, three-dimensional (3D) bioprinting is also a desirable technique since strides can be generated within highly organized tissues recapitulating the *in vivo* architecture of the myocardium [125]. In 2017, in a pioneer work, a printable conductive bioink was developed by incorporating GNRs in GelMA hydrogels for printing 3D cardiac tissues (Fig. 2Ea) [126]. The GNR concentration was optimized to generate a low viscous nanocomposite bioink allowing for the integration of cells into the bioink. NRVMs and cFBs were successfully encapsulated within the bioink and printed to engineer the organized cardiac tissue (Fig. 2Eb). The printed conductive cardiac tissue presented enhanced expression of Cx-43 and sarcomeric α-actinin, improved cell adhesion, and organization, along with enhanced synchronized contraction (Fig. 2Ec and d) [126].

Although it has been hypothesized that GNPs might create conductive bridges across the biomaterials and enhance the electrical signal propagation [115, 123], the mechanism by which these nanomaterials contribute to improved function and maturation of cTE has not been thoroughly and mechanistically investigated. To address this knowledge gap, recently, the Nikkhah group incorporated conductive GNRs and non-conductive silica nanoparticles with approximately similar sizes into GelMA hydrogel to examine the effect of conductivity of nanoparticles on functionalities and maturation of cardiac tissues. Surprisingly, in both nanoengineered hydrogels (*i.e.*, conductive vs. non-conductive), enhanced cell retention and expression of Cx-43, sarcomeric α-actinin, and cTnI were observed, suggesting that conductivity of the scaffold per se is not the only parameter by which the GNRs contribute to the enhancement of functionalities of the ECTs. Nano-scale roughness as well as the mechanical properties of the scaffolds are the other key parameters which influence the biological function of cardiac cells [127]. Due to the undeniable influence of the mechanical properties of the scaffolds on cells, in another work, a biocompatible hybrid biomaterial was developed by incorporating GNRs into collagen hydrogel (GNR-Col) [128]. The GNR-Col scaffold with appropriate stiffness properties (7.25 ± 0.08 kPa) efficiently regulated intercalated disc assembly and formation in the cultured NRVMs. Further mechanistic studies showed that the improved formation of intercalated discs was partly associated with the ILK/p-AKT/GATA4 pathway mediated by β1 integrin. Admittedly, improved β1 integrin expression was also previously shown in the work of Navaei et al., demonstrating that GNRs could activate the mechanical pathway [119]. However, more studies are required in this area to delineate the detailed mechanism of improved functionalities of ECTs in the presence of GNPs. In addition, the majority of the previous studies in this regard have relied on the use of rat-derived CMs. To that end, more work is needed to assess the role of GNPs in biological response (*i.e.*, protein and gene expression), maturation, and contractility of hPSC-CMs.

2.2. Silicon-derived nanomaterials

Silicon nanoparticles have been introduced for diverse applications in drug delivery and tissue engineering [129]. Their meso-porous structure allows pre-loading the nanoparticles with drugs, growth factors, and other molecules of interest that enhance their interaction with cells and engineered tissues [130]. However, one of the most attractive features of silicon nanomaterials has been the possibility of adjusting their electroconductive properties by introducing small impurities (dopants) in their lattice structure [131]. Particularly, due to their size, morphology, optical and electroconductive properties, silicon nanowires (SiNWs) have been of recent interest for the fabrication of ECTs. For instance, Rotenberg et al. created a hybrid system utilizing SiNWs internalized by neonatal rat myofibroblasts and CMs to introduce optical pacing and investigate cellular electrical coupling of the cells (Fig. 3Aa–c) [132]. When light pulses were applied to the hybrid myofibroblasts-SiNWs (MF-SiNWs), it was possible to indirectly stimulate and pace adjacent CMs in *in vitro* cocultures. Additionally, it was demonstrated that injection of MF-SiNWs in the native cardiac tissue was well tolerated, without significant signs of fibrotic encapsulation (Fig. 3Ad). With this, the authors demonstrated that it is possible to integrate minimally invasive optoelectrical silicon-based nanomaterials for cardiac tissue engineering applications.

Mei's group utilized SiNWs for the fabrication of scaffold-free ECTs. Specifically, electroconductive SiNWs (eSiNWs) with a diameter of 100nm and length of 10 μm (Fig. 3Ba) were used along with hiPSC-CMs into the fabrication of cardiac spheroids [133]. To achieve this, a suspension of hiPSC-CMs and eSiNWs (1:1) was created and deposited in agarose microwells. The low-adhesive surface of the agarose promotes cellular aggregation, resulted in a composite microtissue, with eSiNWs located in the intercellular space (Fig. 3Bb). The electroconductive microenvironment created by the addition of the eSiNWs promoted enhanced cellular structures (Fig. 3Bc), denoted by increased expression of sarcomeric α-actinin, Cx-43, and β-myosin heavy chain. Additionally, higher synchronization of spontaneous contraction and increased sarcomere alignment were attributed to the addition of eSiNWs. In a subsequent study of the authors, it was shown that the combination of eSiNWs and external chronic electrical stimulation (2.5V/cm, 1Hz, 5ms) resulted in the formation of more mature cardiac spheroids (Fig. 3Ca–c) [134]. Enhanced expression of the genes involved in the contractile machinery of hiPSC-CMs (*i.e.*, MYH7, increased MYH7/MYH6 ratio, and MYL2) was observed, along with improved cell-cell junction formation, measured by expression of Cx-43 and N-cadherin (Fig. 3Cd). It was speculated that increased availability of cell-cell junction proteins would lead to better engraftment to the native myocardium. However, the size of these microtissues was limited by oxygen and nutrient diffusion [135]. Thus, delivery and treatment of largely affected injured areas could be a challenging task.

Despite the advantages and significance of SiNWs, their *in vivo* application and use need to be thoroughly investigated. For example, biodegradation and clearance pathways of silicon and silicon-derived nanoparticles need to be investigated in detail. Additionally, morphology, size, mesostructure, surface chemistry, among several other features, need to be carefully optimized to avoid acute cytotoxicity and bioaccumulation in non-targeted organs [136].

2.3. Carbon-based nanomaterials (CBNs)

Nanosize carbon allotropes, including carbon nanotubes (CNTs), graphene-based nanosheets, carbon nanohorns, and carbon nanofibers, collectively known as carbon-based nanomaterials (CBNs), have been famous for their outstanding properties. Owing to their mechanical, topological, and electrical properties, this group of materials have gathered significant attention in tissue engineering applications [112, 137–140]. For example, a recognized avenue to address the need for electroactive features in engineering tissues such as cardiac, muscle, and the nerve is incorporating CBNs in commonly used non-conductive biomaterials [139, 141, 142]. In other words, including CBNs into tissue-engineered scaffolds is a facile one-step approach to confer refined properties such as higher physical strength, biological activity, and conductivity to the bulk material, which ultimately can direct cells to form electrically conductive networks [138, 143]. In this section, the recent advances in the application of CBNs to engineering scaffolds to mimic the myocardium microenvironment and ultimately replace infarcted heart tissue are discussed.

CNTs known as cylindrical hollow nanostructures with diameters ranging from below 1 to 100 nm [138, 141] have shown great potential in the maturation of CMs [144–146]. In a work by Martinelli et al., the cultured NRVMs on multi-wall carbon nanotubes (MWCNTs) substrates showed enhanced viability, proliferation, and electrophysiological properties [144]. It was demonstrated that MWNTs significantly improved expression of sarcoplasmic reticulum Ca2+ ATPase 2a cardiac-specific markers (*i.e.*, Cx-43 and sar comeric α-actinin) in NRVMs and functional syncytia. These improvements endowed by CNTs could also safeguard the ECT against pathological hypertrophy, modeled by phenylephrine treatment [146]. One step further, it was demonstrated that the incorporation of CNTs in GelMA hydrogel formed fibril-like bridges between scaffold pores [143, 145] that provided higher mechanical and electrical properties. In addition, the engineered CNT-embedded scaffolds imparted higher adhesion of NRVMs on the nanocomposite film, more uniform 2D cell distribution, higher cell retention and viability, and cell alignment index [145, 147]. Notably, CNTs inclusion (1 mg/mL) also led to enhanced electrophysiological characteristics in terms of higher spontaneous beating rates, while the excitation threshold for NRVMs cultured on hybrid CNT-GelMA was 85% lower in comparison to the control condition (pristine GelMA). CNTs also affect the CMs phenotype demonstrating higher expression of sarcomeric α-actinin and cTnI and better-distributed Cx-43 enhancing contractile features of cultured tissue [145, 147]. The work by Shin et al. demonstrated that incorporated CNTs pre-served cardiac tissue function against heptanol (that disrupts gap-junctions and synchronized beating) up to 60 min by providing a non-cellular network for electrical signal propagation in the GelMA matrix [145]. It has also been reported that the aligned CNTs in GelMA hydrogel could induce cardiac differentiation of mouse stem cell-derived embryoid bodies that were further promoted by an external electrical stimulation [148].

Another family member of CBNs, a powerful counterpart for CNTs in reconstructing electroactive tissues, particularly myocardium, is graphene-based nanosheets [149, 150]. This group of nanomaterials, including graphene (G), graphene oxide (GO), and reduced form of graphene oxide (rGO) nanosheets, is formed of a single layer of carbon atoms connected in the form of 2D hexagonal honeycomb lattice [112, 151, 152]. Like

CNT, the graphene family has been demonstrated to improve mechanical and electrical properties while supporting cellular function within cardiac tissues [153–156]. It has been demonstrated that the NRVMs cultured on rGO-GelMA hydrogel had enhanced cardiac function in comparison to GelMA and even GO-GelMA hydrogel sheets, proved by higher cardiac marker expression, higher spontaneous beating rate, and stronger contraction [143]. Notably, only the cardiac construct on rGO-GelMA showed a response to the external electrical stimulation. These observations have been attributed to the lower electrical resistance in hydrogels incorporated by rGO and the higher ability of rGO in protein absorption compared to GO, which enhances cellular adhesion [143, 150]. In a recent study, the insertion of graphene, as the most conductive material among CBNs, in collagen resulted in enhanced expression of MF20 (sarcomeric myosin) and cTnT (cardiac troponin T) in murine embryonic stem cell-derived CMs and led to significantly higher metabolic activity [149]. To draw a comparison between these siblings, 2D cell seeding on GO-GelMA substrates displayed faster 3T3 fibroblast attachment and higher cell spreading with polygonal shapes than CNT-GelMA films. This observation was attributed to the 2D topological characteristics of GO and higher surface roughness, compared to the 1D shape of CNTs, which dictates the cells' focal adhesion points and sizes [157]. However, in a recently published study by Lee et al., it was revealed that NRVMs cultured on CNT- and rGO-GelMA compared to GO-GelMA thin films showed higher elongation and more local alignment with closer morphology to cardiac muscle cells and enhanced expression of cardiac markers (Fig. 4Aa–c) [143]. Even though the authors have noted a few reasons for this observation, more detailed and mature investigations are required to uncover the underlying mechanisms affecting cell behaviors. In an interesting approach, the electrophysiological features of cardiac tissues developed on CBN nanocomposites were evaluated by measuring spontaneous action potential. The authors demonstrated that the NRVMs matured on CNT-GelMA films had expressed more ventricular phenotypes (assessed by depolarization and repolarization pattern) (Fig. 4Ad), which is of great demand as MI is usually followed by ventricular dysfunction. From a conductivity perspective, the sheet resistance of rGO biohybrid scaffolds (~1 kΩ/sq.) was shown to be approximately 100 times lower than CNT counterparts (~100 kΩ/sq.) [143]. However, compared to graphene, studies denoted that the percolation threshold of CNT nanocomposites is about 85% lower than that of the graphene-based nanocomposite, implying that CNTs provide much higher electrical conductivity than graphene nanosheets with the same loading content [158–160]. Nevertheless, the best conductivity has been achieved when a combination of CNT and graphene nanosheets was applied [161, 162]. This hybridization strategy also helps with higher mechanical properties and lower agglomeration [151, 163]. Therefore, we anticipate that future studies will focus on engineering bio-constructs as cardiac patches based on hybridizing CNT and graphene-based nanosheets to provide higher mechanical and electrical properties.

Recognizing the native myocardium as a flexible and stiff tissue with nanofibrous architecture has drawn great attention for the fabrication of electrospun fibrous mats recapitulating proper structural, mechanical, and electrophysiological characteristics of the native myocardium. In order to achieve these features, CBNs have been incorporated in a wide range of biocomposites including poly(glycerol-sebacate) gelatin (PGS-gelatin) [164],

CHI-poly(vinyl alcohol) [165], silk [166–168], poly(ester-amide)-CHI [169], PCL-CHI-PPy [170]. The inclusion of 1.5% GelMA-coated CNTs within nanofibrous scaffold caused a significant improvement in mechanical toughness (7-fold) and finer fibers with an improved orientation that mimics the anisotropic architecture of the myocardium [164]. From a biological perspective, better CMs alignment and lower excitation threshold (3.5-fold), higher cell viability, and cardiac-specific markers (*i.e.*, Cx-43 and sarcomeric α-actinin) expression were observed in the effect of CNT incorporation [164–166, 168]. Regardless of these improvements, there was still a big difference between the diameter of fabricated nanofibrous scaffolds (ranging between 200 to 400 nm) and the diameter of fiber-like native myocardium (10–100 nm). Therefore, studies evaluating the effect of fiber diameter in the range closer to the native tissue are highly desired. Moreover, the thickness of the developed electrospun scaffolds was significantly lower than that of the infarcted tissue that needs to be replaced. Therefore, future studies are encouraged to focus on the layer-by-layer assembly strategies to stack the living electrospun mats together to get closer to the infarct thickness. In a similar context, inspired by the gradual transition of fiber alignment within the native myocardium (from endocardium to epicardium), Ma's group developed CNT-incorporated nanofiber networks within a GelMA hydrogel shell (Fig. 4Ba–c) [167]. They could ultimately achieve a two-layer network interwoven with an orthogonal orientation, with a multitude of cell layers having a gradual orientation transition (Fig. 4Bd and e). Further studies developing CBN-embedded scaffolds to mimic the native architecture and their *in vivo* function are still in high demand. To this end, bio-fabrication techniques such as 3D bioprinting with the potential to place cells and materials in a precise 3D high resolution with complex architecture can be of great interest.

2.4. Electroconductive polymers (ECPs)

In addition to incorporating conductive nanomaterials within scaffolds, several works that have relied on ECPs in the engineering of cardiac tissues. In this section, we will review the key ECPs which have been specifically used in engineering cardiac tissue constructs. Polypyrrole (PPy), Polyaniline (PANI), and poly(3,4-ethylene dioxythiophene) polystyrene sulfonate (PEDOT:PSS) have been some of the most common ECPs which have been extensively used in several biomedical applications [171–175]. The structure of these ECPs contains conjugated π electron systems allowing for tuning their electrical properties. To that end, the ability to tune the electrical conductivity of scaffolds attracted tremendous attention, specifically in tissue engineering [110, 175–178]. Their electroconductive nature makes them useful for neuronal and cardiac related studies [179, 180]. Specifically, the addition of ECPs can better recapitulate the native cardiac tissue microenvironment by improving scaffold electrical properties and conductive cellular network formation [171, 178, 179, 181]. The following sections focus on the recent progress in utilizing ECPs to enhance cellular (*i.e.*, expression of cardiac biomarkers, CM maturation) and tissue-level properties (*i.e.*, beating, conduction velocities, Ca wave propagation) of scaffolds meant for cTE applications.

PANI is an attractive type of ECP for cTE due to its ease of synthesis, cost efficiency, and proper stability [182]. However, PANI suffers from limited cell-binding motifs and loss of conductivity in prolonged culture conditions [183–185]. Bidez et al. showed the efficacy of

PANI film for adhesion and proliferation of cardiac H9c2 myoblast while maintaining its conductivity up to100 h in the culture medium [186]. However, integration of PANI into soft cardiac tissues is limited because of its biodegradability and inflexibility features [142, 184, 187]. To address this limitation, PANI has been blended with other polymers such as gelatin [185], PCL [187], polyurethane (PU) [188], polylactic acid (PLA) [171], poly(lactic-co-glycolic acid) (PLGA) [189], and PGS [190, 191]. PANI/PLA scaffolds made by either uniaxial and coaxial electrospinning not only promoted adhesion but could also modulate the shape of NRVCs [192]. Similarly, Wang et al. observed partially aligned and well-connected sarcomeric structures on electrospun PANI/PLA scaffolds (Fig. 5A) [171]. Alternatively, blending PANI/PU/PGS was demonstrated to result in scaffolds with well-interconnected pores (> 150 μm) with suitable compression moduli and mechanical strength for the culture of CMs [188]. Within this blended scaffold, even without electrical stimulation, NRVMs cultured on the conductive substrates expressed higher cardiac-specific genes (*i.e.*, actin alpha 4 and troponin T-2) than non-conductive scaffolds and controls. Similarly, Hu et al. developed elastic and electroactive PGS-co-aniline trimer films (Fig. 5Ba) [190]. These micropatterned (*i.e.*, 50/50 μm groove/ridge dimension) films promoted synchronous calcium transients in cultured NRVMs. Enhanced expression of cardiac-specific markers (sarcomeric α-actinin and Cx-43) and improved cell alignment and elongation along the patterned surface were also observed that could support anisotropy of cultured CMs (Fig. 5Bc and d). In addition to blending, another viable strategy to improve the properties of PANI scaffold is by various polymer doping [189, 193, 194]. For instance, Hsiao et al. fabricated electrospun meshes of conductive scaffolds comprised of PANI and poly(lactic-co-glycolic acid) (PLGA) followed by HCl doping (Fig. 5Ca) [189]. The doped meshes acquired positive charges, thereby electrostatically attracting negatively charged laminin and fibronectin proteins that in turn enhanced cell adhesion, supported synchronous beating of cultured NRVMs with an improved expression of Cx-43 and sarcomeric α-actinin (Fig 5Cb and c).

The other widely used ECPs in tissue engineering applications is PPy [98, 181, 195]. Previous studies have shown that PPy is amenable to surface modification (*i.e.*, bioactive molecule functionalization), supports neuron, fibroblast, and endothelial cell adhesion and proliferation and exhibits biocompatibility both *in vitro* and *in vivo* [196–199]. These features have motivated utilizing PPy conductive scaffolds in cTE and myocardial repair applications [180, 200, 201]. However, the poor mechanical properties initially made it difficult to use PPy for scaffold fabrication [180, 195, 202]. To address these challenges, several research groups have tuned the concentration of PPy polymer blends to balance conductivity, biodegradability, and mechanical strength [142, 181, 200, 201]. PPy composite scaffolds have been shown to improve conduction of action potentials, CM proliferation, cell-cell communication, as well as expression of Cx-43 gap junctions [181, 196, 203]. Similarly, incorporating PPy into other scaffolds such as PCL/gelatin [181] and PCL [204] has been shown to improve calcium wave propagation velocities and lower calcium transient duration in 2D CM cultures. Various strategies could be utilized to make composite polymers of PPy with improved properties [205–207]. For example, Tsui et al. developed electroconductive acid-modified silk fibroin- PPy (AMSF + PPy) substrates [207]. Nanosized grooves and ridges were patterned using composite biomaterials

to recapitulate the ECM of the native myocardium. Human embryonic stem cell (hESC)-derived CMs cultured on patterned AMSF + PPy substrates exhibited improved sarcomere development and intracellular organization. Furthermore, CMs cultured on AMSF + PPy substrates with the nanoscale topographical cues demonstrated a greater degree of Cx-43 expression. In contrast, improved troponin expression was not observed in the absence of PPy in the cells cultured on the substrates, even with topographical cues.

PEDOT:PSS is another type of ECP used in cTE [208–210]. For example, Roshanbinfar et al. developed hydrogels made from collagen, alginate, and PEDOT:PSS mimicking ECM fibular structures of the native myocardium [210]. The engineered scaffold exhibited improved electroactivity and promoted the maturation of NRVMs. Specifically, cells cultured on the conductive composite hydrogels showed enhanced expression of Cx-43, improved synchronous beating, enhanced contraction amplitude. Also, the engineered hydrogel improved the beating properties and cell maturation when used with hiPSC-CMs.

In general, it appears that ECPs hold great promise in cTE applications; however, several challenges still persist. For example, to better mimic the mechanical properties and flexibility of the native myocardial tissue, the mechanical features of ECPs, including stiffness, need to be well-tuned. Specifically, PANI is not a flexible polymer [142, 180, 187, 191], and PPy is challenging to handle due to its mechanical properties and brittleness [142, 180, 181, 195, 202]. As discussed earlier, blending them with other polymers has been successfully shown to enhance their material characteristics for the development of engineered tissues. The clinical application of these polymers is also limited due to their solubility, toxicity, and limited host tissue integration [171, 172, 174]. Many studies using ECPs rely on evaluating the behavior of CM monolayers cultured on thin substrates or electrospun sheets [171, 180, 192, 193, 211]. Methods need to be developed to recapitulate the 3D microenvironment of the native myocardial tissue for successful clinical translation of the fabricated conductive tissue. Additionally, converting from a conductive to a non-conductive form upon contact with the physiological or culture medium is a significant obstacle towards the application of these ECPs in tissue engineering [182]. To address this issue, for instance, Mawad et al. immobilized PANI doped phytic acid on CHI films, generating a thin conductive patch that retained its electronic stability in the physiological medium for more than two weeks [212]. Therefore, new strategies are still required to promote the stability and electroactivity of ECP over the construct’s lifetime for long-term applications in bioelectronic devices and tissue engineering scaffolds.

3. *In vivo* applications of electroconductive biomaterials for MI treatment

Over the past two decades, injectable/transplantable biomaterials or patches have been widely investigated for the treatment of MI. Injectable natural biomaterials such as fibrin [43], collagen [46], alginate [213], and CHI [54] have resulted in improved cardiac function, increased LV wall thickness, neovascularization, reduced scar size, and decreased fibrosis [214]. Similarly, there has been also numerous synthetic polymers composed of PNIPAAm [24, 90, 93, 215–217] and PEG [76, 79, 82, 84]. Biomaterials should be engineered based on specific criteria, such as material selection (*i.e.*, biocompatibility, biodegradability), mechanical properties, chemical properties, etc., to lead to the desired outcome. A detailed

explanation of various types of biomaterials has been reviewed elsewhere [214]. However, electrical conductivity has often been underestimated in designing biomaterials specifically for *in vivo* treatment of MI. The application of conductive biomaterials for treating MI stems from the fact that they may enhance the propagation of electrical signals throughout the non-conductive scar tissues [218, 219]. This section summarizes the leading studies on the use of electroconductive biomaterials and their roles in cardiac regeneration after MI *in vivo* (summarized in Table 1).

Similar to *in vitro* studies, PPy has been extensively used for designing conductive biomaterials for MI treatment. In one of the earlier works, a blend of PPy with alginate was used for *in vivo* myocardial regeneration. Intramyocardial injection of the synthesized conductive polymer blend into the infarcted zone of rat hearts induced arteriogenesis and increased the migration of myofibroblasts into the injured zone without any significant inflammation upon five weeks post-injection when compared with the untreated and PBS-treated groups [202]. However, despite these improvements, the infarct size was not significantly different across the experimental groups five weeks post-injection. These improvements were partially attributed to the electrical conductivity of PPy as it could trigger differentiation of the cells responsible for arteriole formation and restore the conduction within the infarcted tissue [202]. Despite promising outcomes, the underlying mechanism of such functional improvements was not further studied.

Due to its biocompatibility [220], CHI has been extensively used as the base polymer for developing conductive injectable/transplantable biomaterials. In 2015, Mihic et al. tested the efficacy of grafting pyrrole to CHI to generate a semi-conductive hydrogel (PPy:CHI) for *in vitro* and *in vivo* studies [219]. NRVMs cultured on PPy:CHI resulted in enhanced Ca^{2+} signal conduction compared with pristine CHI. Cell-free injection of PPy:CHI into the border zone of injured tissue 1-week of post-infarct, improved cardiac contractile function and conduction velocity measured eight weeks after hydrogel injection. Compared with the saline control, the scar size was significantly reduced in biomaterial treated hearts; while, no significant difference between CHI and PPy:CHI groups was observed [219]. However, electrical impulse propagation through the damaged zone was not investigated. In 2018, in another study using a cryoinjury model, intramyocardial injection of PPy:CHI into the injured region of the heart, seven days post-injury, enhanced electrical signals propagation across the infarcted tissue and improved cardiac function without inducing arrhythmias at four weeks post-injection [200]. In these two studies, the efficacy of PPy:CHI hydrogel was successfully shown once injected around the border zone or into the scar area; however, the detailed mechanism of action of the proposed hydrogel requires a further look. In a follow-up study, the same group investigated the mechanism by which the conductive PPy:CHI improves cardiac function [218]. In an *in vitro* model, synchronous contractions were induced in isolated clusters of NRVMs cultured on PPy:CHI hydrogels. Furthermore, intramyocardial delivery of PPy:CHI into fibrotic tissue seven days post-injury induced angiogenesis, reduced scar size, and enhanced cardiac function at three months post-injection without causing any arrhythmias. These improvements were mainly attributed to the enhanced conduction velocity across the fibrotic scar tissue due to the delivery of PPy:CHI hydrogels, leading to cardiac synchronized contraction.

Wang et al. used a dopamine crosslinker to distribute PPy nanoparticles into GelMA and poly(ethylene glycol) diacrylate (PEGDA) hydrogels to form a cryogel (Fig. 6Aa and b) [221]. The incorporated PPy nanoparticles (DOPA-based MA-G/PEGDA/PPY cryogel) resulted in increased Cx-43 and sarcomeric α-actinin expression in cultured NRVMs and enhanced synchronous contracting of the conductive engineered cardiac patch *in vitro* (Fig. 6Ac and d). After being cultured with DiI-labeled NRVMs for eight days, cardiac patches were sutured onto the epicardium of infarcted rat hearts. Transplantation of the engineered patch resulted in enhanced cardiac function, reduced scar size, and improved electric conduction within the infarcted zone at four weeks post-implantation. Furthermore, immunofluorescence (IF) staining of sarcomeric α-actinin was performed to assess the cardiomyogenic effects of the implanted cardiac patches. As indicated (Fig. 6Ae–i), DOPA-based MA-G/PEGDA/PPy cryogel was able to retain a higher number of delivered NRVMs four weeks post-transplantation, confirmed by DiI^+ CMs. It was speculated that PPy nanoparticles might have migrated from the donor patch and fused into the surface of the native CMs, similar to what they observed within *in vitro* experiments [221]. The migration of PPy nanoparticles was similar to another study [222], where CNTs transferred from the scaffold into the host tissue and CMs *in vivo*.

Cardiac patch transplantation and intramyocardial injection of injectable biomaterials could alleviate the adverse effects after MI. However, each approach has its unique benefits, and full regeneration may not be achieved through a single approach. To that end, in a work by Wu et al., a conductive injectable hydrogel along with a self-adhesive cardiac patch were simultaneously administered to the injured heart in a combinatorial approach [223]. Specifically, the bioadhesive hydrogel contained a mixture of dopamine-modified polypyrrole (DA-PPy) and gelatin-dopamine (GelDA) (GelDA/DA-PPy). In contrast, the injectable hydrogel was synthesized by a reaction between hydrazided hyaluronic acid (HHA) and oxidized sodium hyaluronic acid (HA-CHO) (HA-CHO/HHA). Intramyocardial injection of HA-CHO/HHA hydrogel and painting the electroconductive GelDA/DA-PPy hydrogel on the damaged tissue surface resulted in improved expression of Cx-43 and sarcomeric α-actinin, improved cardiac function, thicker LV wall, and enhanced angiogenesis upon four weeks post-injection.

In 2019, Song et al. developed a surgical suture using thermal plastic poly(glycolic acid) (PGA) coated with PPy, which could form an elastically conductive 3D network termed as biospring (Fig. 6Ba and b) [224]. *In vitro* culture of CMs on the biosprings resulted in increased sarcomeric α-actinin and Cx-43 expression and formation of elongated and aligned sarcomeres (Fig. 6Bc and d). Injection of biosprings (16 biosprings per injection) into the infarcted regions increased angiogenesis and reduced infarct size at four weeks post-injection. Compared with sham and non-conductive spring groups, injection of DOPA-coated PPy/PGA resulted in more sarcomeric α-actinin and Cx-43 positive CMs in the scar area (Fig. 6Be1,h2). It was speculated that the conductive 3D biosprings mediate the propagation of electrical signals from the healthy tissues into the infarcted tissue.

Although GNPs have been extensively used for cTE *in vitro*, they have rarely been used for *in vivo* MI treatment. In 2018, Hosoyama et al. tested the efficacy of incorporating GNSs into a collagen-based cardiac patch for *in vitro* biological studies and *in vivo* cardiac

repair applications [225]. *In vitro* culture of NRVMs on the cardiac patch resulted in enhanced expression of Cx-43 under electrical stimulation. Transplantation of the patch into the infarcted mouse hearts via fibrin sealant seven days post MI resulted in reduced scar size, enhanced expression of Cx-43, and sarcomeric α-actinin, as well as increased vasculogenesis within the infarcted area without inducing any ventricular tachycardia at 28 days post-transplantation.

In a different attempt, a conductive injectable hydrogel was developed with equivalent stiffness to native myocardium by grafting poly-3-amino-4-methoxybenzoic acid (PAMB) onto non-conductive gelatin followed by crosslinking via carbodiimide (PAMB-G) [226]. Injection of the hydrogel into the scar area of rat hearts at 1-week post-injury resulted in enhanced cardiac function, reduced scar size, and a thicker LV wall without inducing arrhythmias. It was speculated that injection of PAMB-G hydrogel enhanced propagation of electrical impulse across the scar tissue and helped activation of viable contracting regions within the scar. Recently, a conductive cardiac patch was also developed with equivalent conductivity to native myocardium comprised of a gelatin-based gelfoam grafted with PAMB for the repair of infarcted rat heart [227]. One week post-injury, the epicardial delivery of the cardiac patch loaded with NRVMs significantly improved cardiac function, enhanced propagation of electrical impulse, and reduced the arrhythmias upon four weeks of transplantation.

GO has also been extensively used to introduce electroconductivity features into the designed biomaterials for MI treatment. Paul et al. developed a soft GelMA-based injectable hydrogel to deliver functionalized GO sheets with vascular endothelial growth factor-165 (VEGF) pro-angiogenic gene (fGO_{VEGF}/GelMA) for transfection of infarcted myocardium [228]. In a rat model of acute MI, injection of the proposed nano-complexed hydrogel in the peri-infarct regions resulted in mitotic activities of endothelial cells, enhanced capillary density of myocardium, decreased scar size, and enhanced cardiac function at two weeks post-injection compared with the infarcted hearts injected with other experimental groups (*i.e.*, sham, GelMA alone, fGO_{VEGF}/GelMA). Although this study showed the efficacy of GO for myocardial gene delivery, the specific role of the GO conductivity was not assessed or isolated on overall improved cardiac function. To that end, despite the benefits of the proposed nano-complexed angiogenic hydrogel, the long-term impact of GO should be further evaluated in the host system [228]. Similarly, Zhou et al. designed an electroconductive injectable hydrogel by incorporating GO nanoparticles into oligo(poly(ethylene glycol) fumarate) (OPF) hydrogels [229]. The combination of GO and OPF hydrogels enhanced cell attachment *in vitro*. In a rat MI model, in addition to mechanical support, injection of the conductive OPF/GO hydrogels into the infarct zone resulted in improved Ca^{2+} signal propagation, upregulation of Cx-43 expression, reduced infarct size, and enhanced neovascularization compared with OPF and PBS groups. In 2017, for the first time, Bao et al. developed a soft hydrogel by synthesizing a multi-armed PEGDA700-Melamine (PEG-MEL) using π-π conjugation ring [230]. PEG-MEL was later crosslinked with thiol modified hyaluronic acid (HA-SH) (PEG-MEL/HA-SH). GO was further used to introduce electrical features to the designed hydrogel (PEG-MEL/HA-SH/GO). In a rat model of MI, intramyocardial injection of adipose tissue-derived stromal cells (ADSCs), combined with the proposed conductive hydrogel, resulted in

enhanced expression of Cx-43, improved heart function, thicker LV wall, and reduced scar at four weeks post-injection compared with sham, PBS, PEG-MEL/HA-SH, PEG-MEL/HA-SH/GO, and PEG-MEL/HA-SH/ADSCs groups. Despite the positive outcome of this study, GO nanoparticles' metabolism and biosafety are still a major concern upon injection into the damaged myocardium. To address this issue, the same group utilized tetraaniline (TA) in a recent study to partly enhance conductivity within the synthesized hydrogel while maintaining its biocompatibility [231]. Michael addition was used for the reaction of tetraaniline-polyethylene glycol diacrylate (TA-PEG) and thiolated hyaluronic acid (HA-SH) to generate a compliant hydrogel (TA-PEG/HA-SH) with conductivity resembling the native myocardium. They tested the efficacy of the proposed combinatorial approach towards heart repair by intramyocardial transplantation of the conductive hydrogel encapsulated with ADSCs and plasmid DNA encoding endothelial nitric oxide synthase (eNOs) nanocomplexes. The proposed approach promoted cardiac function, increased Cx-43 and sarcomeric α-actinin expression, reduced infarct size, and increased vessel density at four weeks post-transplantation. In addition, although the beneficial effects of the plasmid on neovascularization were demonstrated, the transgene's expression time should be controlled in future endeavors. In these two studies, including PEG-MEL/HA-SH/GO/ADSCs [230] and TA-PEG/HA-SH [231], hydrogel treated hearts showed enhanced α-smooth muscle actin (α-SMA) expression across the damaged zone. The authors speculated that the improved cardiac function has resulted from the increased population of fibroblasts within the infarcted region, promoting the transduction of mechanical signals within the myocardium. However, expansion of cFBs is not necessarily beneficial as they could differentiate into myofibroblasts and increase fibrosis within the scar tissue [232].

In another study, a thermosensitive injectable hydrogel was developed by incorporating single-wall carbon nanotubes (SWCNTs) into PNIAPAAm hydrogel to improve bioactivities and adhesion of PNIAPAAm to encapsulated cells [85]. Preliminary *in vitro* studies demonstrated the PNIPAAm/SWCNTs hydrogel efficacy in promoting proliferation and adhesion of encapsulated brown adipose-derived stem cells (BASCs). Furthermore, intramyocardial delivery of BASCs-laden PNIPAAm/SWCNTs enhanced cells' retention within the infarct region compared with PBS/BASCs group at one week post-injection. Four weeks post-transplantation, BASCs were differentiated to CMs, resulting in improved cardiac function and reduced scar size in PNIPAAm/SWCNTs/BASCs experimental group.

Despite innovative approaches and promising outcomes, shown in previous studies, with the use of injectable conductive biomaterials or transplantation of patches for the treatment of MI, the mechanism of action of these materials needs to be further studied. Multiple mechanisms have been speculated for the effect of conductive biomaterials in improved cardiac function and tissue regeneration *in vivo*. Some studies proposed that the improvements were partially attributed to the conductivity feature of the conductive biomaterials, which may promote electrical propagation across the scar regions as it can trigger the migration of cells into the infarct region and restoring the conduction of the infarcted tissue [200, 218, 223, 226, 227, 231] Electrical signal propagation within the cardiac muscle undergoes significant changes after MI. Specifically, after MI, the formation of fibrotic tissue causes disconnection of functioning and beating CMs resulting in delayed electrical signal propagation and the loss of tissue synchronicity [218]. To better investigate

this mechanism, recently, He et al. designed an experiment to explain how electroconductive biomaterial (*i.e.*, CHI-PPy) could act as a wire to restore electrical signal propagation within non-conductive and fibrotic scar tissue after MI [218]. They specifically assessed the energy loss and latency time of the generated electrical signals by heart tissue passing through an equivalent circuit *in vitro*. It was found that the latency time was 5-fold shorter for electroconductive CHI-PPY groups compared to the non-conductive gelatin groups confirming higher conduction velocity within the conductive biomaterials. In addition, electrical signal energy upon passing through the conductive CHI-PPY biomaterial was more than 2 times higher than the non-conductive gelatin. Injection of CHI-PPY into scar tissue resulted in reduced impedance and enhanced electrical conductivity. Specifically, higher field potential amplitude was observed in the scar tissue of the CHI-PPy injected hearts compared to the damaged hearts injected with nonconductive CHI. Moreover, microelectrode array analyses indicated that current failed to re-enter the scar region in non-conductive CHI-injected hearts, while in the conductive CHI-PPy injected hearts, the electroconductive signals well propagated throughout the scar region. Compared to CHI injected hearts, faster conduction velocity and reduced resistivity of the PPy-CHI injected hearts were also confirmed. Overall, the generated current by myocardium faced less resistance, and the energy loss was significantly lower in CHI-PPY injected hearts compared to the non-conductive injected group [218].

In another study, Zhou et al. constructed three-dimensional conductive ECTs (c-ECT) by incorporating SWCNTs into gelatin hydrogel scaffolds to provide a conducive microenvironment for cTE *in vitro* [222]. Cell-laden c-ECTs were sutured onto the rat hearts' epicardial surface at two weeks post-infarct. Four weeks after implantation, the c-ECTs were integrated into the host myocardium, which led to the migration of transplanted SWCNTs and CMs into the scar regions. The formation of well-aligned cell bundles, and enhanced expression of N-cadherin and Cx-43 compared with sham and gelatin groups, were evident. The authors hypothesized that SWCNTs might have helped the fusion of c-ECTs into the host tissues while triggering the native heart cells to migrate into the infarcted areas. Additionally, the authors demonstrated infiltration of vasculature from the host tissue into the transplanted constructs one week after implantation. From a mechanistic point of view, the authors found that the expression levels of β1-integrin, ILK, p-AKT, and β-catenin were higher within the c-ECT groups compared with sham and non-conductive groups suggesting the possible activation of ILK/Akt-catenin pathway in the infarcted zone. Four weeks post-transplantation, CD68 positive macrophages were also shown to accumulate in the myocardium's scar area. Therefore, it deserves further investigation to delineate whether infiltration of macrophages contributed to the positive outcome of the engineered c-ECT.

An essential criterion of biomaterial-based heart regeneration after MI is to develop a less invasive approach for the delivery of the engineered biomaterials [214]. Conductive materials have been applied to the infarcted hearts primarily through direct intramyocardial injection or suturing of patches onto the epicardial surface. Through intramyocardial injection, the amount of injected biomaterial could be controlled in a minimally invasive approach. However, in preclinical studies using large animals (*e.g.*, porcine), multiple injections are required to evenly distribute the biomaterial into the infarcted tissue [37]. Some biomaterials could also be delivered into the epicardial surface in the form of

cardiac patches. Cardiac patches are advantageous because they could deliver more cells and therapeutic agents and mechanically support the LV wall [233]. However, cardiac patch delivery often requires invasive surgical procedures (*i.e.*, suturing) that could increase the likelihood of inflammatory responses [234]. Multiple innovative strategies have been successfully developed recently to address these issues. For instance, in 2016, a suture-free technique was created to transplant cardiac patches through light illumination (photoadhesion) [212]. Specifically, a bioadhesive cardiac patch was fabricated by adding a photoactivated dye (*i.e.*, Rose Bengal) into a CHI film (Fig. 7Aa–d). The bioadhesive cardiac patch was then successfully transplanted onto the epicardium surface after exposure to green laser (λ = 532 nm) without any need for suturing. Two weeks post-transplantation, the cardiac patches remained firmly adhered to the heart tissues, confirming the viability and efficacy of this method for delivery of cardiac patches in a minimally invasive fashion (Fig. 7Ae and f). In 2018, Tal Dvir's group developed another suture-free technique to transplant cardiac patches into the heart tissues [235]. In this study, a cardiac patch composed of albumin electrospun fibers and GNRs was developed, loaded with cardiac cells (Fig. 7Ba–c). The cardiac patches were positioned on the rat epicardium surface and exposed to a near-infrared (IR) laser (808 nm). It was suggested that the GNRs converted the absorbed light into thermal energy, changing the molecular structure of the fibrous scaffold, which firmly adhered it to the wall of the heart (Fig. 7Bd–f). Although this approach was promising and innovative, the safety of the procedure for clinical cardiac therapy of patients could be further studied.

In another attempt, Liang et al. developed an adhesive paintable conductive hydrogel that could be painted on the surface of the epicardium in the form of a patch, avoiding the need for suturing or light exposure (Fig. 7C) [234]. This paintable conductive biomaterial was designed by two-step Michael addition reactions to sequentially introduce pyrrole groups and dopamine. First, the reaction of pentaerythritol triacrylate (PETA), dopamine hydrochloride, and PEGDA resulted in a hyperbranched poly(amino ester) polymer (HPAE). The second Michael addition step was performed to react the pyrrole monomer with acrylate groups of HPAE resulted in a conductive bioadhesive polymer (HPAE-Py). To this hyperbranched polymer, gelatin was further added to enhance the biocompatibility of the precursor solution. Fe^{3+} as a multifunctional curing agent was then used to initiate the polymerization of pyrrole groups. The dopamine-Fe^{3+} introduced bioadhesive feature while the PPy formed *in situ* introduced conductivity to the biomaterial. The delivered hydrogel (HPAE-Py/Gelatin) to the infarcted hearts infiltrated and fused within the host tissue and firmly bonded to the beating heart within four weeks post-delivery. Compared to sham and HPAE/Gelatin groups, the conductive adhesive patch (HPAE-Py/Gelatin) resulted in reduced scar size and fibrosis, thicker LV wall, improved expression of Cx-43, and increased generation of new vessels within the scar tissue.

4. Advantages and disadvantages of the electroconductive components for cTE

Electroconductive biomaterials have widely been used in various tissue engineering disciplines from neural [236], skeletal [237], to cardiac [142]. As reviewed above, the

use of electroconductive elements such as GNPs, CBNs, or ECPs has been the key strategy to promote electrical signal propagation and conductivity within engineered tissues. The synthesized electroconductive scaffolds need to fulfill specific requirements, such as cytocompatibility and acceptable biodegradation rate, to successfully support the functionalities of engineered tissue. However, there are certain advantages or disadvantages associated with the use of each approach which will be briefly discussed below.

GNPs have been favorable for the use in cTE due to their acceptable biocompatibility, controllable size, and shape fabrication [238]. As an advantage, GNPs are biocompatible and could be synthesized in different geometries and sizes, such as nanospheres, nanorods, and nanowires. However, the effect of GNPs geometry and size on functionalities of ECTs remained to be mechanistically investigated. The electroconductivity features of the resultant scaffolds also depend on the type of GNPs and the base polymer. For instance, GNRs (average length, ~60 nm) when incorporated into alginate hydrogels did not impart a significant improvement in terms of electroconductivity compared to the pristine alginate [115]. On the other hand, when GNWs (average length, ~1.0 μm) were incorporated into the same hydrogel, a significant increase in electrical current was detected [115]. In contrast, the electroconductivity of GelMA hydrogel was significantly promoted when incorporated with GNRs (average length, ~50 nm) [119,124,127] as functional of nanomaterial concentration. Although cytocompatibility of GNPs has been confirmed in several publications, their cytotoxicity has been shown to be dose-dependent [239] which poses a limitation in tuning the electroconductivity of the final synthesized scaffolds. Furthermore, incorporation of GNPs results in scaffolds with low mechanical strength compared to CBNs, where the lack of homogenous dispersion within the base hydrogel material may also limit specific applications that require high concentrations of these nanomaterials [238].

Similar to GNPs, CBNs have also been extensively used in cTE for both *in vitro* and *in vivo* applications. However, CBNs pose potential issues such as hydrophobicity that may result in aggregation once incorporated into the base hydrogel materials [240]. CNBs cytotoxicity yet remains to be another challenge that may lead to host immune reaction upon *in vivo* transplantation of the engineering tissues [142]. CBNs also appear in various shapes, sizes, and geometries that impact their toxicity. For example, the biocompatibility of graphene and its derivatives has been reported to depend on their concentration, shapes, and number of layers [241, 242]. To that end, more investigations are required to unveil their side effects upon *in vivo* applications. In addition, the biodistribution of these nanomaterials (GNPs, CBNs) and accumulation within other organs upon injection have led to arguments over their safe use for clinical applications.

Apart from the key nanomaterials (GNRs, CBNs), ECPs such as PANI, PPy, and PEDOT:PSS have been widely used in cTE. In general, ECPs have been shown to have poor biocompatibility [243], while their conductivity characteristics also decline over time within the physiological environment [182]. According to previous studies, the biocompatibility of ECPs is also dose-dependent. For instance, 30% PPy in PCL and gelatin was shown to exhibit cytotoxic effects [181]. Although there are certain benefits with the use of ECPs for engineering functional cardiac tissues, the long-term degradation rate, cytotoxicity, and carcinogenic effects may limit their clinical application for the treatment of injured

myocardium [238]. In addition, the current knowledge regarding the potential immune response of the implanted ECPs *in vivo* is limited. In-depth mechanistic investigations are required to address the remained questions in this regard.

Owing to the inherent biocompatibility and degradation issues of the abovementioned electroconductive nanomaterials and polymers, recently, more attention has been devoted towards the development of new generation of biocompatible and electroconductive materials for cTE. For instance, in a recent study, He et al. synthesized a naturally aligned self-conductive cellulose-based scaffold from sea squirt, named tunic hydrogel, for cTE application (Fig. 8Aa) [244]. The self-conductive hydrogel was further doped with PPy (PTC hydrogel) to enhance its electroconductivity (Fig. 8Aa and b). The pristine tunic hydrogel, tunic hydrogel, and PTC hydrogel showed uniform current distribution; however, the current and conductivity within the tunic and PTC hydrogels were stronger than the pristine tunic hydrogel (Fig. 8Ac). NRVMs, after cultured for 7 days on the tunic and PTC hydrogels, showed improved orientation, enhanced Cx-43 and sarcomeric α-actinin expression compared to the pristine tunic control hydrogel (Fig. 8Ad). Transplantation of the cell-laden cardiac patches fabricated from the tunic and PTC hydrogels into the rat infarcted hearts resulted in enhanced cardiac function, increased ventricle wall thickness and reduced infarct size, and angiogenesis. In addition, enhanced expression of Cx-43 and more organized sarcomeric α-actinin were observed within the patch transplantation site. Although PPy doping was shown to enhance the electroconductivity of self-conductive tunic hydrogel, it may still pose safety issues due to its non-biodegradability and side effects upon *in vivo* implantation. However, the tunic hydrogel itself with suitable conductivity could be a promising candidate for MI repair with minimal side effects.

In another recent work, Song et al. incorporated hydrophilic ionic polymer, namely polyacrylic acid (PAA), into oxidized alginate (OA)/gelatin (Geln) (OG) hydrogel to develop a porous ionic conductive hydrogel, named $POG_{1,}$ with appropriate biocompatibility and electrical conductivity ($35.36 \pm 7.72 \times 10^{-3}$ S/cm) equiva lent to the native human heart tissues [240]. The ionic conductive hydrogel could be advantageous over traditional electroconductive components for cTE as they maintain electroconductivity under strains condition, avoiding the disconnection of electroconductive paths. Furthermore, this new class of the synthesized hydrogel introduced a homogenous electroconductivity within the scaffold without aggregated conductive phases, as opposed to the use of other traditional electroconductive materials (*i.e.*, PPy, rGO, and CNT) (Fig. 8Ba). Compared to the non-conductive OG and CNT-OG with inhomogeneous conductivity, NRVMs cultured on the POG_1 hydrogel exhibited minimal cytotoxicity, significantly oriented and elongated sarcomeric α-actinin structure, enhanced Cx-43 expression (Fig. 8Bb), and improved synchronization. Notably, in a rat model of MI, implantation of cell-laden POG_1 engineered cardiac patches resulted in suppression of cardiac fibrosis (Fig. 8Bc), increased LV wall thickness, and improved cardiac function compared to control MI and OG groups at four weeks post-transplantation. The formation of new blood vessels is also a crucial factor for oxygen and nutrients supply within the infarct region for treatment of MI [245]. Several *in vivo* studies have reported the formation of angiogenesis within the infarct zone after injection of conductive hydrogels [202, 218, 224, 229, 231] or transplantation of conductive cardiac patches [212, 222, 225]. Similar to previous studies, in this work, transplantation

of engineered POG_1 cardiac patches into the infarcted rat hearts resulted in angiogenesis within the scar tissue confirmed by immunostaining for vWF (micro-vessels) and α-SMA (arterioles) markers (Fig. 8Bd) [240].

5. Conclusions and future directions

Engineered scaffolds or biomaterials that incorporate electrical cues may provide the cells with the necessary conducive microenvironment, resembling the native myocardium, for the formation of functional cardiac tissues *in vitro*. Over the past decade, various conductive materials, including GNPs, silicon-derived nanomaterials, CBNs, and ECPs, have been successfully utilized to endow electroconductivity features to semi- and non-conductive biocompatible materials (either natural or synthetic) for enhanced cTE and cardiac regeneration after MI. The idea of injecting conductive biomaterials into the scar area stems from the fact that the electroconductive biomaterial could electrically connect the isolated CMs across the scar tissue. However, the remaining viable CMs in the scar area might not be sufficient for full regeneration of the infarcted hearts. One possible solution could be the delivery of exogenous CMs via injectable conductive biomaterials. Although cell delivery has been shown to have beneficial effects to some extent, the maturation level of the injected CMs, the risk of immune rejection, and tumor formation are still a big concern [17]. To that end, an appropriately designed acellular biomaterial could provide the cells in the infarcted tissue with a new microenvironment to promote regeneration and electrical signal propagation, avoiding the risks associated with cell-based therapies [246]. Furthermore, ECM protein engineering approaches [247] could be practiced to develop conductive ECM-based biomaterials for the effective delivery of CM proliferation cues such as agrin, which has been recently found as a stimulator for CM proliferation [248]. Therefore, a combined strategy for developing conductive acellular injectable or implantable scaffolds for the proliferation of resident CMs could be a new approach for enhanced cardiac regeneration. Additionally, there exist some gaps in this field that are worthy of further investigation. Despite the advancements of the field and extensive reports on the beneficial impact of the hybrid conductive materials on cultured CMs, further mechanistic studies are needed to unravel the underlying molecular mechanisms that potentially influence the native-like structures and functionalities of the engineered tissues as well as molecular signatures of CMs such as protein and gene expression. Apart from mechanistic biological knowledge gaps, the fate and biodistribution of the conductive nanomaterials *in vivo* should be further unveiled. Moreover, the electroconductivity properties of the designed tissue constructs diminish in the physiologic environment [182]. Although previous studies have successfully investigated the electroconductivity up to two weeks [212], further attempts are required to design electroconductive biomaterials with long-term effects for potential *in vivo* applications with enhanced efficacy. In the native tissue, cells are located in an ECM with a complex composition; however, most of the designed cardiac tissues incorporate only one or two ECM components. It has been shown that a multicomponent ECM scaffold could efficiently differentiate stem cells towards cardiomyogenic fate [249]. One possible route could be endowing electrical features to the cardiac tissues generated from an optimized combination of ECM proteins. Therefore, a conductive biomaterial with

appropriate electrical and ECM cues (*i.e.*, protein and biochemical composition) could enhance the functionalities of the cTE toward translational applications.

Aknowledgments

MN would like to acknowledge the NSF Award # 2016501, Arizona Biomedical Research Commission (ABRC) New Investigator Award # AWD32676 and NIH Award # 1R21EB028396-01. AM would like to acknowledge funding by the Institution Funding Program—King Abdulaziz University—Kingdom of Saudi Arabia, award number IFPRC-005-135-202.

References

[1]. W.H. OrganizationWorld Health Statistics 2016: Monitoring Health for the SDGs Sustainable Development Goals, World Health Organization, 2016.

[2]. Deshmukh V, Wang J, Martin JF, Leading progress in heart regeneration and repair, Curr. Opin. Cell Biol 61 (2019) 79–85. [PubMed: 31408771]

[3]. Benjamin EJ, Blaha MJ, Chiuve SE, Cushman M, Das SR, Deo R, de Ferranti SD, Floyd J, Fornage M, Gillespie C, Isasi CR, Jimenez MC, Jordan LC, Judd SE, Lackland D, Lichtman JH, Lisabeth L, Liu S, Longenecker CT, Mackey RH, Matsushita K, Mozaffarian D, Mussolino ME, Nasir K, Neumar RW, Palaniappan L, Pandey DK, Thiagarajan RR, Reeves MJ, Ritchey M, Rodriguez CJ, Roth GA, Rosamond WD, Sasson C, Towfighi A, Tsao CW, Turner MB, Virani SS, Voeks JH, Willey JZ, Wilkins JT, Wu JH, Alger HM, Wong SS, Muntner P, American C Heart Association Statistics, S. Stroke Statistics, Heart disease and stroke statistics-2017 update: a report from the American Heart Association, Circulation 135 (10) (2017) e146–e603. [PubMed: 28122885]

[4]. Murry CE, Reinecke H, Pabon LM, Regeneration gaps: observations on stem cells and cardiac repair, J. Am. Coll. Cardiol 47 (9) (2006) 1777–1785. [PubMed: 16682301]

[5]. Bergmann O, Zdunek S, Felker A, Salehpour M, Alkass K, Bernard S, Sjostrom SL, Szewczykowska M, Jackowska T, Dos Remedios C, Malm T, Andra M, Jashari R, Nyengaard JR, Possnert G, Jovinge S, Druid H, Frisen J, Dynamics of cell generation and turnover in the human heart, Cell 161 (7) (2015) 1566–1575. [PubMed: 26073943]

[6]. Prabhu SD, Frangogiannis NG, The biological basis for cardiac repair after myocardial infarction: from inflammation to fibrosis, Circ. Res 119 (1) (2016) 91–112. [PubMed: 27340270]

[7]. Patino-Guerrero A, Veldhuizen J, Zhu W, Migrino RQ, Nikkhah M, Three-dimensional scaffold-free microtissues engineered for cardiac repair, J. Mater. Chem. B 8 (34) (2020) 7571–7590. [PubMed: 32724973]

[8]. Perin EC, Borow KM, Silva GV, DeMaria AN, Marroquin OC, Huang PP, Traverse JH, Krum H, Skerrett D, Zheng Y, Willerson JT, Itescu S, Henry TD, A phase II dose-escalation study of allogeneic mesenchymal precursor cells in patients with ischemic or nonischemic heart failure, Circ. Res 117 (6) (2015) 576–584. [PubMed: 26148930]

[9]. Cambria E, Pasqualini FS, Wolint P, Günter J, Steiger J, Bopp A, Hoer-strup SP, Emmert MY, Translational cardiac stem cell therapy: advancing from first-generation to next-generation cell types, NPJ Regen. Med 2 (1) (2017) 1–10. [PubMed: 29302338]

[10]. Lee RT, Adult cardiac stem cell concept and the process of science, Circulation 138 (25) (2018) 2940–2942. [PubMed: 30566005]

[11]. Chien KR, Frisén J, Fritsche-Danielson R, Melton DA, Murry CE, Weiss-man IL, Regenerating the field of cardiovascular cell therapy, Nat. Biotechnol 37 (3) (2019) 232–237. [PubMed: 30778231]

[12]. Shiba Y, Fernandes S, Zhu WZ, Filice D, Muskheli V, Kim J, Palpant NJ, Gantz J, Moyes KW, Reinecke H, Van Biber B, Dardas T, Mignone JL, Izawa A, Hanna R, Viswanathan M, Gold JD, Kotlikoff MI, Sarvazyan N, Kay MW, Murry CE, Laflamme MA, Human ES-cell-derived cardiomyocytes electrically couple and suppress arrhythmias in injured hearts, Nature 489 (7415) (2012) 322–325. [PubMed: 22864415]

[13]. Chong JJ, Yang X, Don CW, Minami E, Liu YW, Weyers JJ, Mahoney WM, Van Biber B, Cook SM, Palpant NJ, Gantz JA, Fugate JA, Muskheli V, Gough GM, Vogel KW, Astley CA, Hotchkiss CE, Baldessari A, Pabon L, Reinecke H, Gill EA, Nelson V, Kiem HP, Laflamme MA, Murry CE, Human embryonic-stem-cell-derived cardiomyocytes regenerate non-human primate hearts, Nature 510 (7504) (2014) 273–277. [PubMed: 24776797]

[14]. Ye L, Chang YH, Xiong Q, Zhang P, Zhang L, Somasundaram P, Lepley M, Swingen C, Su L, Wendel JS, Guo J, Jang A, Rosenbush D, Greder L, Dutton JR, Zhang J, Kamp TJ, Kaufman DS, Ge Y, Zhang J, Cardiac repair in a porcine model of acute myocardial infarction with human induced pluripotent stem cell-derived cardiovascular cells, Cell Stem Cell 15 (6) (2014) 750–761. [PubMed: 25479750]

[15]. Shiba Y, Gomibuchi T, Seto T, Wada Y, Ichimura H, Tanaka Y, Ogasawara T, Okada K, Shiba N, Sakamoto K, Ido D, Shiina T, Ohkura M, Nakai J, Uno N, Kazuki Y, Oshimura M, Minami I, Ikeda U, Allogeneic transplantation of iPS cell-derived cardiomyocytes regenerates primate hearts, Nature 538 (7625) (2016) 388–391. [PubMed: 27723741]

[16]. Nguyen PK, Neofytou E, Rhee JW, Wu JC, Potential strategies to address the major clinical barriers facing stem cell regenerative therapy for cardiovascular disease: a review, JAMA Cardiol. 1 (8) (2016) 953–962. [PubMed: 27579998]

[17]. Berry JL, Zhu W, Tang YL, Krishnamurthy P, Ge Y, Cooke JP, Chen Y, Garry DJ, Yang HT, Rajasekaran NS, Koch WJ, Li S, Domae K, Qin G, Cheng K, Kamp TJ, Ye L, Hu S, Ogle BM, Rogers JM, Abel ED, Davis ME, Prabhu SD, Liao R, Pu WT, Wang Y, Ping P, Bursac N, Vunjak-Novakovic G, Wu JC, Bolli R, Menasche P, Zhang J, Convergences of life sciences and engineering in understanding and treating heart failure, Circ. Res 124 (1) (2019) 161–169. [PubMed: 30605412]

[18]. Eulalio A, Mano M, Dal Ferro M, Zentilin L, Sinagra G, Zacchigna S, Giacca M, Functional screening identifies miRNAs inducing cardiac regeneration, Nature 492 (7429) (2012) 376–381. [PubMed: 23222520]

[19]. Wang LL, Liu Y, Chung JJ, Wang T, Gaffey AC, Lu M, Cavanaugh CA, Zhou S, Kanade R, Atluri P, Morrisey EE, Burdick JA, Local and sustained miRNA delivery from an injectable hydrogel promotes cardiomyocyte proliferation and functional regeneration after ischemic injury, Nat Biomed Eng 1 (2017) 983–992. [PubMed: 29354322]

[20]. Liu B, Lee BW, Nakanishi K, Villasante A, Williamson R, Metz J, Kim J, Kanai M, Bi L, Brown K, Di Paolo G, Homma S, Sims PA, Topkara VK, Vunjak-Novakovic G, Cardiac recovery via extended cell-free delivery of extracellular vesicles secreted by cardiomyocytes derived from induced pluripotent stem cells, Nat. Biomed. Eng 2 (5) (2018) 293–303. [PubMed: 30271672]

[21]. Pal A, Vernon BL, Nikkhah M, Therapeutic neovascularization promoted by injectable hydrogels, Bioact Mater. 3 (4) (2018) 389–400. [PubMed: 30003178]

[22]. Karam J-P, Muscari C, Sindji L, Bastiat G, Bonafè F, Venier-Julienne M-C, Montero-Menei NC, Pharmacologically active microcarriers associated with thermosensitive hydrogel as a growth factor releasing biomimetic 3D scaffold for cardiac tissue-engineering, J. Controll. Release 192 (2014) 82–94.

[23]. Guo HD, Cui GH, Yang JJ, Wang C, Zhu J, Zhang LS, Jiang J, Shao SJ, Sustained delivery of VEGF from designer self-assembling peptides improves cardiac function after myocardial infarction, Biochem. Biophys. Res. Commun 424 (1) (2012) 105–111. [PubMed: 22732415]

[24]. Wall ST, Yeh CC, Tu RY, Mann MJ, Healy KE, Biomimetic matrices for myocardial stabilization and stem cell transplantation, J. Biomed. Mater. Res. Part A 95 (4) (2010) 1055–1066.

[25]. Salimath AS, Phelps EA, Boopathy AV, Che PL, Brown M, García AJ, Davis ME, Dual delivery of hepatocyte and vascular endothelial growth factors via a protease-degradable hydrogel improves cardiac function in rats, PLoS One 7 (11) (2012) e50980. [PubMed: 23226440]

[26]. Bhutani S, Nachlas AL, Brown ME, Pete T, Johnson CT, García AJ, Davis ME, Evaluation of hydrogels presenting extracellular matrix-derived adhesion peptides and encapsulating cardiac progenitor cells for cardiac repair, ACS Biomater. Sci. Eng 4 (1) (2018) 200–210. [PubMed: 29457128]

[27]. Nelson DM, Hashizume R, Yoshizumi T, Blakney AK, Ma Z, Wagner WR, Intramyocardial injection of a synthetic hydrogel with delivery of bFGF and IGF1 in a rat model of ischemic cardiomyopathy, Biomacromolecules 15 (1) (2014) 1–11. [PubMed: 24345287]

[28]. Wang Z, Long DW, Huang Y, Chen WCW, Kim K, Wang Y, Decellularized neonatal cardiac extracellular matrix prevents widespread ventricular remodeling in adult mammals after myocardial infarction, Acta Biomater. 87 (2019) 140–151. [PubMed: 30710713]

[29]. Sonnenberg SB, Rane AA, Liu CJ, Rao N, Agmon G, Suarez S, Wang R, Munoz A, Bajaj V, Zhang S, Braden R, Schup-Magoffin PJ, Kwan OL, DeMaria AN, Cochran JR, Christman KL, Delivery of an engineered HGF fragment in an extracellular matrix-derived hydrogel prevents negative LV remodeling post-myocardial infarction, Biomaterials 45 (2015) 56–63. [PubMed: 25662495]

[30]. Efraim Y, Sarig H, Cohen Anavy N, Sarig U, de Berardinis E, Chaw SY, Krishnamoorthi M, Kalifa J, Bogireddi H, Duc TV, Kofidis T, Baruch L, Boey FYC, Venkatraman SS, Machluf M, Biohybrid cardiac ECM-based hydrogels improve long term cardiac function post myocardial infarction, Acta Biomater. 50 (2017) 220–233. [PubMed: 27956366]

[31]. Francis MP, Breathwaite E, Bulysheva AA, Varghese F, Rodriguez RU, Dutta S, Semenov I, Ogle R, Huber A, Tichy AM, Chen S, Zemlin C, Human placenta hydrogel reduces scarring in a rat model of cardiac ischemia and enhances cardiomyocyte and stem cell cultures, Acta Biomater. 52 (2017) 92–104. [PubMed: 27965171]

[32]. Seif-Naraghi SB, Singelyn JM, Salvatore MA, Osborn KG, Wang JJ, Sampat U, Kwan OL, Strachan GM, Wong J, Schup-Magoffin PJ, Safety and efficacy of an injectable extracellular matrix hydrogel for treating myocardial infarction, Sci. Transl. Med 5 (173) (2013) 173ra25–173ra25.

[33]. Cao J, Poss KD, The epicardium as a hub for heart regeneration, Nat. Rev. Cardiol 15 (10) (2018) 631–647. [PubMed: 29950578]

[34]. Khan M, Nickoloff E, Abramova T, Johnson J, Verma SK, Krishnamurthy P, Mackie AR, Vaughan E, Garikipati VN, Benedict C, Ramirez V, Lambers E, Ito A, Gao E, Misener S, Luongo T, Elrod J, Qin G, Houser SR, Koch WJ, Kishore R, Embryonic stem cell-derived exosomes promote endogenous repair mechanisms and enhance cardiac function following myocardial infarction, Circ. Res 117 (1) (2015) 52–64. [PubMed: 25904597]

[35]. Gallet R, Dawkins J, Valle J, Simsolo E, de Couto G, Middleton R, Tseliou E, Luthringer D, Kreke M, Smith RR, Marban L, Ghaleb B, Marban E, Exosomes secreted by cardiosphere-derived cells reduce scarring, attenuate adverse remodelling, and improve function in acute and chronic porcine myocardial infarction, Eur. Heart J 38 (3) (2017) 201–211. [PubMed: 28158410]

[36]. Cutts J, Nikkhah M, Brafman DA, Biomaterial approaches for stem cell-based myocardial tissue engineering: supplementary issue: stem cell biology, Biomark. Insights 10 (2015) 77–90. [PubMed: 26052226]

[37]. Johnson TD, Christman KL, Injectable hydrogel therapies and their delivery strategies for treating myocardial infarction, Expert Opin. Drug Deliv 10 (1) (2013) 59–72. [PubMed: 23140533]

[38]. Peña B, Laughter M, Jett S, Rowland TJ, Taylor MR, Mestroni L, Park D, Injectable hydrogels for cardiac tissue engineering, Macromol. Biosci 18 (6) (2018) 1800079.

[39]. Segers VF, Lee RT, Biomaterials to enhance stem cell function in the heart, Circ. Res 109 (8) (2011) 910–922. [PubMed: 21960724]

[40]. Reis L, Chiu LL, Feric N, Fu L, Radisic M, in: Injectable Biomaterials for Cardiac Regeneration and Repair, Cardiac Regeneration and Repair, Elsevier, 2014, pp. 49–81.

[41]. Williams C, Budina E, Stoppel WL, Sullivan KE, Emani S, Emani SM, Black LD, Cardiac extracellular matrix–fibrin hybrid scaffolds with tunable properties for cardiovascular tissue engineering, Acta Biomater. 14 (2015) 84–95. [PubMed: 25463503]

[42]. Christman KL, Vardanian AJ, Fang Q, Sievers RE, Fok HH, Lee RJ, Injectable fibrin scaffold improves cell transplant survival, reduces infarct expansion, and induces neovasculature formation in ischemic myocardium, J. Am. Coll. Cardiol 44 (3) (2004) 654–660. [PubMed: 15358036]

[43]. Christman KL, Fok HH, Sievers RE, Fang Q, Lee RJ, Fibrin glue alone and skeletal myoblasts in a fibrin scaffold preserve cardiac function after myocardial infarction, Tissue Eng. 10 (3–4) (2004) 403–409. [PubMed: 15165457]

[44]. Yu J, Christman KL, Chin E, Sievers RE, Saeed M, Lee RJ, Restoration of left ventricular geometry and improvement of left ventricular function in a rodent model of chronic ischemic cardiomyopathy, J. Thorac. Cardiovasc. Surg 137 (1) (2009) 180–187. [PubMed: 19154923]

[45]. Rinkevich-Shop S, Landa-Rouben N, Epstein FH, Holbova R, Feinberg MS, Goitein O, Kushnir T, Konen E, Leor J, Injectable collagen implant improves survival, cardiac remodeling, and function in the early period after myocarditis in rats, J. Cardiovasc. Pharmacol. Ther 19 (5) (2014) 470–480. [PubMed: 24572032]

[46]. Dai W, Wold LE, Dow JS, Kloner RA, Thickening of the infarcted wall by collagen injection improves left ventricular function in rats: a novel approach to preserve cardiac function after myocardial infarction, J. Am. Coll. Cardiol 46 (4) (2005) 714–719. [PubMed: 16098441]

[47]. Kuraitis D, Berardinelli MG, Suuronen EJ, Musarò A, A necrotic stimulus is required to maximize matrix-mediated myogenesis in mice, Dis. Models Mech 6 (3) (2013) 793–801.

[48]. Blackburn NJ, Sofrenovic T, Kuraitis D, Ahmadi A, McNeill B, Deng C, Rayner KJ, Zhong Z, Ruel M, Suuronen EJ, Timing underpins the benefits associated with injectable collagen biomaterial therapy for the treatment of myocardial infarction, Biomaterials 39 (2015) 182–192. [PubMed: 25468370]

[49]. Reis LA, Chiu LL, Liang Y, Hyunh K, Momen A, Radisic M, A peptide-modified chitosan–collagen hydrogel for cardiac cell culture and delivery, Acta Biomater. 8 (3) (2012) 1022–1036. [PubMed: 22155066]

[50]. Xu G, Wang X, Deng C, Teng X, Suuronen EJ, Shen Z, Zhong Z, Injectable biodegradable hybrid hydrogels based on thiolated collagen and oligo (acryloyl carbonate)–poly (ethylene glycol)–oligo (acryloyl carbonate) copolymer for functional cardiac regeneration, Acta Biomater. 15 (2015) 55–64. [PubMed: 25545323]

[51]. Suuronen EJ, Veinot JP, Wong S, Kapila V, Price J, Griffith M, Mesana TG, Ruel M, Tissue-engineered injectable collagen-based matrices for improved cell delivery and vascularization of ischemic tissue using CD133+ progenitors expanded from the peripheral blood, Circulation 114 (1_supplement) (2006) I-138–I-144. [PubMed: 16820563]

[52]. Li J, Shu Y, Hao T, Wang Y, Qian Y, Duan C, Sun H, Lin Q, Wang C, A chitosan–glutathione based injectable hydrogel for suppression of oxidative stress damage in cardiomyocytes, Biomaterials 34 (36) (2013) 9071–9081. [PubMed: 24001992]

[53]. Xu B, Li Y, Deng B, Liu X, Wang L, Zhu QL, Chitosan hydrogel improves mesenchymal stem cell transplant survival and cardiac function following myocardial infarction in rats, Exp. Ther. Med 13 (2) (2017) 588–594. [PubMed: 28352335]

[54]. Lu WN, Lü SH, Wang HB, Li DX, Duan CM, Liu ZQ, Hao T, He WJ, Xu B, Fu Q, Functional improvement of infarcted heart by co-injection of embryonic stem cells with temperature-responsive chitosan hydrogel, Tissue Eng. Part A 15 (6) (2009) 1437–1447. [PubMed: 19061432]

[55]. Wang H, Shi J, Wang Y, Yin Y, Wang L, Liu J, Liu Z, Duan C, Zhu P, Wang C, Promotion of cardiac differentiation of brown adipose derived stem cells by chitosan hydrogel for repair after myocardial infarction, Biomaterials 35 (13) (2014) 3986–3998. [PubMed: 24508080]

[56]. Liu Z, Wang H, Wang Y, Lin Q, Yao A, Cao F, Li D, Zhou J, Duan C, Du Z, The influence of chitosan hydrogel on stem cell engraftment, survival and homing in the ischemic myocardial microenvironment, Biomaterials 33 (11) (2012) 3093–3106. [PubMed: 22265788]

[57]. Tormos CJ, Abraham C, Madihally SV, Improving the stability of chitosan–gelatin-based hydrogels for cell delivery using transglutaminase and controlled release of doxycycline, Drug Deliv. Transl. Res 5 (6) (2015) 575–584. [PubMed: 26373948]

[58]. Feyen DA, Gaetani R, Deddens J, van Keulen D, van Opbergen C, Poldervaart M, Alblas J, Chamuleau S, van Laake LW, Doevendans PA, Gelatin microspheres as vehicle for cardiac progenitor cells delivery to the myocardium, Adv. Healthc. Mater 5 (9) (2016) 1071–1079. [PubMed: 26913710]

[59]. Nikkhah M, Akbari M, Paul A, Memic A, Dolatshahi-Pirouz A, Khademhosseini A, Gelatin-based biomaterials for tissue engineering and stem cell bioengineering, Biomater. Nat. Adv. Devices Ther (2016) 37–62.

[60]. Hao T, Li J, Yao F, Dong D, Wang Y, Yang B, Wang C, Injectable fullerenol/alginate hydrogel for suppression of oxidative stress damage in brown adipose-derived stem cells and cardiac repair, ACS Nano 11 (6) (2017) 5474–5488. [PubMed: 28590722]

[61]. Deng B, Shen L, Wu Y, Shen Y, Ding X, Lu S, Jia J, Qian J, Ge J, Delivery of alginate-chitosan hydrogel promotes endogenous repair and preserves cardiac function in rats with myocardial infarction, J. Biomed. Mater. Res. Part A 103 (3) (2015) 907–918.

[62]. Ceccaldi C, Bushkalova R, Alfarano C, Lairez O, Calise D, Bourin P, Frugier C, Rouzaud-Laborde C, Cussac D, Parini A, Evaluation of polyelectrolyte complex-based scaffolds for mesenchymal stem cell therapy in cardiac ischemia treatment, Acta Biomater. 10 (2) (2014) 901–911. [PubMed: 24211733]

[63]. Ruvinov E, Leor J, Cohen S, The promotion of myocardial repair by the sequential delivery of IGF-1 and HGF from an injectable alginate biomaterial in a model of acute myocardial infarction, Biomaterials 32 (2) (2011) 565–578. [PubMed: 20889201]

[64]. Zhao S, Xu Z, Wang H, Reese BE, Gushchina LV, Jiang M, Agarwal P, Xu J, Zhang M, Shen R, Bioengineering of injectable encapsulated aggregates of pluripotent stem cells for therapy of myocardial infarction, Nat. Commun 7 (1) (2016) 1–12.

[65]. Song M, Jang H, Lee J, Kim JH, Kim SH, Sun K, Park Y, Regeneration of chronic myocardial infarction by injectable hydrogels containing stem cell homing factor SDF-1 and angiogenic peptide Ac-SDKP, Biomaterials 35 (8) (2014) 2436–2445. [PubMed: 24378015]

[66]. Yoon SJ, Fang YH, Lim CH, Kim BS, Son HS, Park Y, Sun K, Regeneration of ischemic heart using hyaluronic acid-based injectable hydrogel, J. Biomed. Mater. Res. Part B Appl. Biomater 91 (1) (2009) 163–171.

[67]. Ifkovits JL, Tous E, Minakawa M, Morita M, Robb JD, Koomalsingh KJ, Gorman JH, Gorman RC, Burdick JA, Injectable hydrogel properties influence infarct expansion and extent of postinfarction left ventricular remodeling in an ovine model, Proc. Natl. Acad. Sci 107 (25) (2010) 11507–11512. [PubMed: 20534527]

[68]. Johnson TD, DeQuach JA, Gaetani R, Ungerleider J, Elhag D, Nigam V, Behfar A, Christman KL, Human versus porcine tissue sourcing for an injectable myocardial matrix hydrogel, Biomater. Sci 2 (5) (2014) 735–744.

[69]. Seif-Naraghi SB, Horn D, Schup-Magoffin PA, Madani MM, Christman KL, Patient-to-patient variability in autologous pericardial matrix scaffolds for cardiac repair, J. Cardiovasc. Transl. Res 4 (5) (2011) 545–556. [PubMed: 21695575]

[70]. Williams C, Quinn KP, Georgakoudi I, Black LD, Young developmental age cardiac extracellular matrix promotes the expansion of neonatal cardiomyocytes *in vitro*, Acta Biomater. 10 (1) (2014) 194–204. [PubMed: 24012606]

[71]. Seif-Naraghi SB, Salvatore MA, Schup-Magoffin PJ, Hu DP, Christman KL, Design and characterization of an injectable pericardial matrix gel: a potentially autologous scaffold for cardiac tissue engineering, Tissue Eng. Part A 16 (6) (2010) 2017–2027. [PubMed: 20100033]

[72]. Singelyn JM, Sundaramurthy P, Johnson TD, Schup-Magoffin PJ, Hu DP, Faulk DM, Wang J, Mayle KM, Bartels K, Salvatore M, Catheter-deliverable hydrogel derived from decellularized ventricular extracellular matrix increases endogenous cardiomyocytes and preserves cardiac function post-myocardial infarction, J. Am. Coll. Cardiol 59 (8) (2012) 751–763. [PubMed: 22340268]

[73]. Dobner S, Bezuidenhout D, Govender P, Zilla P, Davies N, A synthetic non-degradable polyethylene glycol hydrogel retards adverse post-infarct left ventricular remodeling, J. Card. Fail 15 (7) (2009) 629–636. [PubMed: 19700140]

[74]. Wang T, Jiang XJ, Tang QZ, Li XY, Lin T, Wu DQ, Zhang XZ, Okello E, Bone marrow stem cells implantation with α-cyclodextrin/MPEG–PCL–MPEG hydrogel improves cardiac function after myocardial infarction, Acta Biomater. 5 (8) (2009) 2939–2944. [PubMed: 19426843]

[75]. Kraehenbuehl TP, Ferreira LS, Zammaretti P, Hubbell JA, Langer R, Cell-responsive hydrogel for encapsulation of vascular cells, Biomaterials 30 (26) (2009) 4318–4324. [PubMed: 19500842]

[76]. Kraehenbuehl TP, Ferreira LS, Hayward AM, Nahrendorf M, Van Der Vlies AJ, Vasile E, Weissleder R, Langer R, Hubbell JA, Human embryonic stem cell-derived microvascular grafts

for cardiac tissue preservation after myocardial infarction, Biomaterials 32 (4) (2011) 1102–1109. [PubMed: 21035182]

[77]. Komeri R, Muthu J, *In situ* crosslinkable elastomeric hydrogel for long-term cell encapsulation for cardiac applications, J. Biomed. Mater. Res. Part A 104 (12) (2016) 2936–2944.

[78]. Rane AA, Chuang JS, Shah A, Hu DP, Dalton ND, Gu Y, Peterson KL, Omens JH, Christman KL, Increased infarct wall thickness by a bio-inert material is insufficient to prevent negative left ventricular remodeling after myocardial infarction, PLoS One 6 (6) (2011) e21571. [PubMed: 21731777]

[79]. Wu J, Zeng F, Huang XP, Chung JCY, Konecny F, Weisel RD, Li RK, Infarct stabilization and cardiac repair with a VEGF-conjugated, injectable hydrogel, Biomaterials 32 (2) (2011) 579–586. [PubMed: 20932570]

[80]. Komeri R, Muthu J, Injectable, cytocompatible, elastic, free radical scavenging and electroconductive hydrogel for cardiac cell encapsulation, Coll. Surf. B Biointerfaces 157 (2017) 381–390.

[81]. Steele AN, Cai L, Truong VN, Edwards BB, Goldstone AB, Eskandari A, Mitchell AC, Marquardt LM, Foster AA, Cochran JR, A novel protein-engineered hepatocyte growth factor analog released via a shear-thinning injectable hydrogel enhances post-infarction ventricular function, Biotechnol. Bioeng 114 (10) (2017) 2379–2389. [PubMed: 28574594]

[82]. Jiang XJ, Wang T, Li XY, Wu DQ, Zheng ZB, Zhang JF, Chen JL, Peng B, Jiang H, Huang C, Injection of a novel synthetic hydrogel preserves left ventricle function after myocardial infarction, J. Biomed. Mater. Res. Part A 90 (2) (2009) 472–477An Official Journal of The Society for Biomaterials, The Japanese Society for Biomaterials, and The Australian Society for Biomaterials and the Korean Society for Biomaterials.

[83]. Chen J, Guo R, Zhou Q, Wang T, Injection of composite with bone marrow-derived mesenchymal stem cells and a novel synthetic hydrogel after myocardial infarction: a protective role in left ventricle function, Kaohsiung J. Med. Sci 30 (4) (2014) 173–180. [PubMed: 24656157]

[84]. Wang T, Jiang XJ, Lin T, Ren S, Li XY, Zhang XZ, Tang QZ, The inhibition of postinfarct ventricle remodeling without polycythaemia following local sustained intramyocardial delivery of erythropoietin within a supramolecular hydrogel, Biomaterials 30 (25) (2009) 4161–4167. [PubMed: 19539990]

[85]. Li X, Zhou J, Liu Z, Chen J, Lü S, Sun H, Li J, Lin Q, Yang B, Duan C, A PNIPAAm-based thermosensitive hydrogel containing SWCNTs for stem cell transplantation in myocardial repair, Biomaterials 35 (22) (2014) 5679–5688. [PubMed: 24746964]

[86]. Peña B, Martinelli V, Jeong M, Bosi S, Lapasin R, Taylor MR, Long CS, Shandas R, Park D, Mestroni L, Biomimetic polymers for cardiac tissue engineering, Biomacromolecules 17 (5) (2016) 1593–1601. [PubMed: 27073119]

[87]. Shi Y, Ma C, Peng L, Yu G, Conductive “smart” hybrid hydrogels with PNIPAM and nanostructured conductive polymers, Adv. Funct. Mater 25 (8) (2015) 1219–1225.

[88]. Tang J, Cui X, Caranasos TG, Hensley MT, Vandergriff AC, Hartanto Y, Shen D, Zhang H, Zhang J, Cheng K, Heart repair using nanogel-encapsulated human cardiac stem cells in mice and pigs with myocardial infarction, ACS Nano 11 (10) (2017) 9738–9749. [PubMed: 28929735]

[89]. Cui H, Liu Y, Cheng Y, Zhang Z, Zhang P, Chen X, Wei Y, *In vitro* study of electroactive tetraaniline-containing thermosensitive hydrogels for cardiac tissue engineering, Biomacromolecules 15 (4) (2014) 1115–1123. [PubMed: 24597966]

[90]. Li XY, Wang T, Jiang XJ, Lin T, Wu DQ, Zhang XZ, Okello E, Xu HX, Yuan MJ, Injectable hydrogel helps bone marrow-derived mononuclear cells restore infarcted myocardium, Cardiology 115 (3) (2010) 194–199. [PubMed: 20145396]

[91]. Ohya S, Nakayama Y, Matsuda T, Material design for an artificial extracellular matrix: cell entrapment in poly (N-isopropylacrylamide)(PNIPAM)-grafted gelatin hydrogel, J. Artif. Org 4 (4) (2001) 308–314.

[92]. Cai L, Dewi RE, Heilshorn SC, Injectable hydrogels with *in situ* double network formation enhance retention of transplanted stem cells, Adv. Funct. Mater 25 (9) (2015) 1344–1351. [PubMed: 26273242]

[93]. Navaei A, Truong D, Heffernan J, Cutts J, Brafman D, Sirianni RW, Vernon B, Nikkhah M, PNIPAAm-based biohybrid injectable hydrogel for cardiac tissue engineering, Acta Biomater. 32 (2016) 10–23. [PubMed: 26689467]

[94]. Anderson RH, Yanni J, Boyett MR, Chandler NJ, Dobrzynski H, The anatomy of the cardiac conduction system, Clin. Anat 22 (1) (2009) 99–113 [PubMed: 18773472] The Official Journal of the American Association of Clinical Anatomists and the British Association of Clinical Anatomists.

[95]. Scanlon VC, Sanders T, Essentials of Anatomy and Physiology, FA Davis, 2018.

[96]. Menasche P, Hagege AA, Vilquin JT, Desnos M, Abergel E, Pouzet B, Bel A, Sarateanu S, Scorsin M, Schwartz K, Bruneval P, Benbunan M, Marolleau JP, Duboc D, Autologous skeletal myoblast transplantation for severe postinfarction left ventricular dysfunction, J. Am. Coll. Cardiol 41 (7) (2003) 1078–1083. [PubMed: 12679204]

[97]. Monteiro LM, Vasques-Novoa F, Ferreira L, Pinto-do OP, Nascimento DS, Restoring heart function and electrical integrity: closing the circuit, NPJ Regen. Med 2 (2017) 9. [PubMed: 29302345]

[98]. Solazzo M, O'Brien FJ, Nicolosi V, Monaghan MG, The rationale and emergence of electroconductive biomaterial scaffolds in cardiac tissue engineering, APL Bioeng. 3 (4) (2019) 041501. [PubMed: 31650097]

[99]. Veldhuizen J, Cutts J, Brafman DA, Migrino RQ, Nikkhah M, Engineering anisotropic human stem cell-derived three-dimensional cardiac tissue on-a-chip, Biomaterials 256 (2020) 120195. [PubMed: 32623207]

[100]. Veldhuizen J, Migrino RQ, Nikkhah M, Three-dimensional microengineered models of human cardiac diseases, J. Biol. Eng 13 (1) (2019) 29. [PubMed: 30988697]

[101]. Zhang B, Korolj A, Lai BFL, Radisic M, Advances in organ-on-a-chip engineering, Nat. Rev. Mater 3 (8) (2018) 257–278.

[102]. Liu W, Zhao L, Wang C, Zhou J, Conductive nanomaterials for cardiac tissues engineering, Eng. Regen 1 (2020) 88–94.

[103]. Dahl SL, Rhim C, Song YC, Niklason LE, Mechanical properties and compositions of tissue engineered and native arteries, Ann. Biomed. Eng 35 (3) (2007) 348–355. [PubMed: 17206488]

[104]. Chaudhuri R, Ramachandran M, Moharil P, Harumalani M, Jaiswal AK, Biomaterials and cells for cardiac tissue engineering: current choices, Mater. Sci. Eng. C 79 (2017) 950–957.

[105]. Zeltinger J, Sherwood JK, Graham DA, Müeller R, Griffith LG, Effect of pore size and void fraction on cellular adhesion, proliferation, and matrix deposition, Tissue Eng. 7 (5) (2001) 557–572. [PubMed: 11694190]

[106]. Badylak SF, Taylor D, Uygun K, Whole-organ tissue engineering: decellularization and recellularization of three-dimensional matrix scaffolds, Annu. Rev. Biomed. Eng 13 (2011) 27–53. [PubMed: 21417722]

[107]. Ott HC, Matthiesen TS, Goh S-K, Black LD, Kren SM, Netoff TI, Taylor DA, Perfusion-decellularized matrix: using nature's platform to engineer a bioartificial heart, Nat. Med 14 (2) (2008) 213–221. [PubMed: 18193059]

[108]. Zimmermann WH, Fink C, Kralisch D, Remmers U, Weil J, Eschenhagen T, Three-dimensional engineered heart tissue from neonatal rat cardiac myocytes, Biotechnol. Bioeng 68 (1) (2000) 106–114. [PubMed: 10699878]

[109]. Cobley CM, Chen J, Cho EC, Wang LV, Xia Y, Gold nanostructures: a class of multifunctional materials for biomedical applications, Chem. Soc. Rev 40 (1) (2011) 44–56. [PubMed: 20818451]

[110]. Kharaziha M, Memic A, Akbari M, Brafman DA, Nikkhah M, Nano-enabled approaches for stem cell-based cardiac tissue engineering, Adv. Healthc. Mater 5 (13) (2016) 1533–1553. [PubMed: 27199266]

[111]. Yi C, Liu D, Fong CC, Zhang J, Yang M, Gold nanoparticles promote osteogenic differentiation of mesenchymal stem cells through p38 MAPK pathway, ACS Nano 4 (11) (2010) 6439–6448. [PubMed: 21028783]

[112]. Mehrali M, Thakur A, Pennisi CP, Talebian S, Arpanaei A, Nikkhah M, Dolatshahi-Pirouz A, Nanoreinforced hydrogels for tissue engineering: biomaterials that are compatible with load-bearing and electroactive tissues, Adv. Mater 29 (8) (2017) 1603612.

[113]. Sridhar S, Venugopal JR, Sridhar R, Ramakrishna S, Cardiogenic differentiation of mesenchymal stem cells with gold nanoparticle loaded functionalized nanofibers, Coll. Surf. B Biointerfaces 134 (2015) 346–354.

[114]. Bursac N, Loo Y, Leong K, Tung L, Novel anisotropic engineered cardiac tissues: studies of electrical propagation, Biochem. Biophys. Res. Commun 361 (4) (2007) 847–853. [PubMed: 17689494]

[115]. Dvir T, Timko BP, Brigham MD, Naik SR, Karajanagi SS, Levy O, Jin H, Parker KK, Langer R, Kohane DS, Nanowired three-dimensional cardiac patches, Nat. Nanotechnol 6 (11) (2011) 720–725. [PubMed: 21946708]

[116]. Gutstein DE, Morley GE, Tamaddon H, Vaidya D, Schneider MD, Chen J, Chien KR, Stuhlmann H, Fishman GI, Conduction slowing and sudden arrhythmic death in mice with cardiac-restricted inactivation of connexin43, Circ. Res 88 (3) (2001) 333–339. [PubMed: 11179202]

[117]. You JO, Rafat M, Ye GJ, Auguste DT, Nanoengineering the heart: conductive scaffolds enhance connexin 43 expression, Nano Lett. 11 (9) (2011) 3643–3648. [PubMed: 21800912]

[118]. Li XP, Qu KY, Zhang F, Jiang HN, Zhang N, Nihad C, Liu CM, Wu KH, Wang XW, Huang NP, High-aspect-ratio water-dispersed gold nanowires incorporated within gelatin methacrylate hydrogels for constructing cardiac tissues *in vitro*, J. Mater. Chem. B 8 (32) (2020) 7213–7224. [PubMed: 32638823]

[119]. Navaei A, Saini H, Christenson W, Sullivan RT, Ros R, Nikkhah M, Gold nanorod-incorporated gelatin-based conductive hydrogels for engineering cardiac tissue constructs, Acta Biomater. 41 (2016) 133–146. [PubMed: 27212425]

[120]. Shevach M, Fleischer S, Shapira A, Dvir T, Gold nanoparticle-decellularized matrix hybrids for cardiac tissue engineering, Nano Lett. 14 (10) (2014) 5792–5796. [PubMed: 25176294]

[121]. Fleischer S, Shevach M, Feiner R, Dvir T, Coiled fiber scaffolds embedded with gold nanoparticles improve the performance of engineered cardiac tissues, Nanoscale 6 (16) (2014) 9410–9414. [PubMed: 24744098]

[122]. Kim DH, Lipke EA, Kim P, Cheong R, Thompson S, Delannoy M, Suh KY, Tung L, Levchenko A, Nanoscale cues regulate the structure and function of macroscopic cardiac tissue constructs, Proc. Natl. Acad. Sci. U. S. A 107 (2) (2010) 565–570. [PubMed: 20018748]

[123]. Shevach M, Maoz BM, Feiner R, Shapira A, Dvir T, Nanoengineering gold particle composite fibers for cardiac tissue engineering, J. Mater. Chem. B 1 (39) (2013) 5210–5217. [PubMed: 32263327]

[124]. Navaei A, Moore N, Sullivan RT, Truong D, Migrino RQ, Nikkhah M, Electrically conductive hydrogel-based micro-topographies for the development of organized cardiac tissues, RSC Adv. 7 (6) (2017) 3302–3312.

[125]. Kang HW, Lee SJ, Ko IK, Kengla C, Yoo JJ, Atala A, A 3D bioprinting system to produce human-scale tissue constructs with structural integrity, Nat. Biotechnol 34 (3) (2016) 312–319. [PubMed: 26878319]

[126]. Zhu K, Shin SR, van Kempen T, Li YC, Ponraj V, Nasajpour A, Mandla S, Hu N, Liu X, Leijten J, Lin YD, Hussain MA, Zhang YS, Tamayol A, Khademhosseini A, Gold nanocomposite bioink for printing 3D cardiac constructs, Adv. Funct. Mater 27 (12) (2017).

[127]. Navaei A, Rahmani Eliato K, Ros R, Migrino RQ, Willis BC, Nikkhah M, The influence of electrically conductive and non-conductive nanocomposite scaffolds on the maturation and excitability of engineered cardiac tissues, Biomater. Sci 7 (2) (2019) 585–595. [PubMed: 30426116]

[128]. Li Y, Shi X, Tian L, Sun H, Wu Y, Li X, Li J, Wei Y, Han X, Zhang J, Jia X, Bai R, Jing L, Ding P, Liu H, Han D, AuNP-Collagen matrix with localized stiffness for cardiac-tissue engineering: enhancing the assembly of intercalated discs by beta1-integrin-mediated signaling, Adv. Mater 28 (46) (2016) 10230–10235. [PubMed: 27723133]

[129]. McInnes S, Voelcker N, Porous silicon–polymer composites for cell culture and tissue engineering applications, in: Porous Silicon for Biomedical Applications, Elsevier, 2014, pp. 420–469.

[130]. Zuidema JM, Dumont CM, Wang J, Batchelor WM, Lu YS, Kang J, Bertucci A, Ziebarth NM, Shea LD, Sailor MJ, Porous silicon nanoparticles embedded in poly (lactic-co-glycolic acid) nanofiber scaffolds deliver neurotrophic payloads to enhance neuronal growth, Adv. Funct. Mater 30 (25) (2020) 2002560. [PubMed: 32982626]

[131]. Schmidt V, Wittemann JV, Senz S, Gösele U, Silicon nanowires: a review on aspects of their growth and their electrical properties, Adv. Mater 21 (25–26) (2009) 2681–2702.

[132]. Rotenberg MY, Yamamoto N, Schaumann EN, Matino L, Santoro F, Tian B, Living myofibroblast–silicon composites for probing electrical coupling in cardiac systems, Proc. Natl. Acad. Sci 116 (45) (2019) 22531–22539. [PubMed: 31624124]

[133]. Tan Y, Richards D, Xu R, Stewart-Clark S, Mani SK, Borg TK, Menick DR, Tian B, Mei Y, Silicon nanowire-induced maturation of cardiomyocytes derived from human induced pluripotent stem cells, Nano Lett. 15 (5) (2015) 2765–2772. [PubMed: 25826336]

[134]. Richards DJ, Tan Y, Coyle R, Li Y, Xu R, Yeung N, Parker A, Menick DR, Tian B, Mei Y, Nanowires and electrical stimulation synergistically improve functions of hiPSC cardiac spheroids, Nano Lett. 16 (7) (2016) 4670–4678. [PubMed: 27328393]

[135]. Tan Y, Richards D, Coyle RC, Yao J, Xu R, Gou W, Wang H, Menick DR, Tian B, Mei Y, Cell number per spheroid and electrical conductivity of nanowires influence the function of silicon nanowired human cardiac spheroids, Acta Biomater. 51 (2017) 495–504. [PubMed: 28087483]

[136]. Gongalsky M, Sviridov A, Bezsudnova YI, Osminkina L, Biodegradation model of porous silicon nanoparticles, Coll. Surf. B Biointerfaces 190 (2020) 110946.

[137]. Talebian S, Mehrali M, Taebnia N, Pennisi CP, Kadumudi FB, Foroughi J, Hasany M, Nikkhah M, Akbari M, Orive G, Self-healing hydrogels: the next paradigm shift in tissue engineering? Adv. Sci 6 (16) (2019) 1801664.

[138]. Hopley EL, Salmasi S, Kalaskar DM, Seifalian AM, Carbon nanotubes leading the way forward in new generation 3D tissue engineering, Biotechnol. Adv 32 (5) (2014) 1000–1014. [PubMed: 24858314]

[139]. Burnstine-Townley A, Eshel Y, Amdursky N, Conductive scaffolds for cardiac and neuronal tissue engineering: governing factors and mechanisms, Adv. Funct. Mater 30 (18) (2020) 1901369.

[140]. Hosoyama K, Ahumada M, Goel K, Ruel M, Suuronen EJ, Alarcon EI, Electroconductive materials as biomimetic platforms for tissue regeneration, Biotechnol. Adv 37 (3) (2019) 444–458. [PubMed: 30797094]

[141]. Veerubhotla K, Lee CH, Emerging trends in nanocarbon-based cardiovascular applications, Adv. Ther 3 (7) (2020) 1900208.

[142]. Ashtari K, Nazari H, Ko H, Tebon P, Akhshik M, Akbari M, Alhosseini SN, Mozafari M, Mehravi B, Soleimani M, Electrically conductive nanomaterials for cardiac tissue engineering, Adv. Drug Deliv. Rev 144 (2019) 162–179. [PubMed: 31176755]

[143]. Lee J, Manoharan V, Cheung L, Lee S, Cha BH, Newman P, Farzad R, Mehrotra S, Zhang K, Khan F, Nanoparticle-based hybrid scaffolds for deciphering the role of multimodal cues in cardiac tissue engineering, ACS Nano 13 (11) (2019) 12525–12539. [PubMed: 31621284]

[144]. Martinelli V, Cellot G, Toma FM, Long CS, Caldwell JH, Zentilin L, Giacca M, Turco A, Prato M, Ballerini L, Carbon nanotubes promote growth and spontaneous electrical activity in cultured cardiac myocytes, Nano Lett. 12 (4) (2012) 1831–1838. [PubMed: 22432413]

[145]. Shin SR, Jung SM, Zalabany M, Kim K, Zorlutuna P, Kim SB, Nikkhah M, Khabiry M, Azize M, Kong J, Carbon-nanotube-embedded hydrogel sheets for engineering cardiac constructs and bioactuators, ACS Nano 7 (3) (2013) 2369–2380. [PubMed: 23363247]

[146]. Martinelli V, Cellot G, Toma FM, Long CS, Caldwell JH, Zentilin L, Giacca M, Turco A, Prato M, Ballerini L, Carbon nanotubes instruct physiological growth and functionally mature syncytia: nongenetic engineering of cardiac myocytes, ACS Nano 7 (7) (2013) 5746–5756. [PubMed: 23734857]

[147]. Pok S, Vitale F, Eichmann SL, Benavides OM, Pasquali M, Jacot JG, Biocompatible carbon nanotube–chitosan scaffold matching the electrical conductivity of the heart, ACS Nano 8 (10) (2014) 9822–9832. [PubMed: 25233037]

[148]. Ahadian S, Yamada S, Ramón-Azcón J, Estili M, Liang X, Nakajima K, Shiku H, Khademhosseini A, Matsue T, Hybrid hydrogel-aligned carbon nanotube scaffolds to enhance cardiac differentiation of embryoid bodies, Acta Biomater. 31 (2016) 134–143. [PubMed: 26621696]

[149]. Ryan AJ, Kearney CJ, Shen N, Khan U, Kelly AG, Probst C, Brauchle E, Biccai S, Garciarena CD, Vega-Mayoral V, Electroconductive biohybrid collagen/pristine graphene composite biomaterials with enhanced biological activity, Adv. Mater 30 (15) (2018) 1706442.

[150]. Shin SR, Zihlmann C, Akbari M, Assawes P, Cheung L, Zhang K, Manoharan V, Zhang YS, Yüksekkaya M, Wan K.t., Reduced graphene oxide-gelMA hybrid hydrogels as scaffolds for cardiac tissue engineering, Small 12 (27) (2016) 3677–3689. [PubMed: 27254107]

[151]. Mehrali M, Bagherifard S, Akbari M, Thakur A, Mirani B, Mehrali M, Hasany M, Orive G, Das P, Emneus J, Blending electronics with the human body: a pathway toward a cybernetic future, Adv. Sci 5 (10) (2018) 1700931.

[152]. Jing X, Mi HY, Napiwocki BN, Peng XF, Turng LS, Mussel-inspired electroactive chitosan/graphene oxide composite hydrogel with rapid self-healing and recovery behavior for tissue engineering, Carbon 125 (2017) 557–570.

[153]. Sekuła-Stryjewska M, Noga S, Dźwigońska M, Adamczyk E, Karnas E, Jagiełło J, Szkaradek A, Chytrosz P, Boruczkowski D, Madeja Z, Graphene-based materials enhance cardiomyogenic and angiogenic differentiation capacity of human mesenchymal stem cells – Focus on cardiac tissue regeneration, Mater. Sci. Eng. C 119 (2021) 111614.

[154]. Zhang F, Zhang N, Meng HX, Liu HX, Lu YQ, Liu CM, Zhang ZM, Qu KY, Huang NP, Easy applied gelatin-based hydrogel system for long-term functional cardiomyocyte culture and myocardium formation, ACS Biomater. Sci. Eng 5 (6) (2019) 3022–3031. [PubMed: 33405656]

[155]. Smith AS, Yoo H, Yi H, Ahn EH, Lee JH, Shao G, Nagornyak E, Laflamme MA, Murry CE, Kim DH, Micro-and nano-patterned conductive graphene–PEG hybrid scaffolds for cardiac tissue engineering, Chem. Commun 53 (53) (2017) 7412–7415.

[156]. Annabi N, Shin SR, Tamayol A, Miscuglio M, Bakooshli MA, Assmann A, Mostafalu P, Sun JY, Mithieux S, Cheung L, Highly elastic and conductive human-based protein hybrid hydrogels, Adv. Mater 28 (1) (2016) 40–49. [PubMed: 26551969]

[157]. Shin SR, Aghaei-Ghareh-Bolagh B, Gao X, Nikkhah M, Jung SM, Dolatshahi-Pirouz A, Kim SB, Kim SM, Dokmeci MR, Tang X, Layer-by-layer assembly of 3D tissue constructs with functionalized graphene, Adv. Funct. Mater 24 (39) (2014) 6136–6144. [PubMed: 25419209]

[158]. Du J, Zhao L, Zeng Y, Zhang L, Li F, Liu P, Liu C, Comparison of electrical properties between multi-walled carbon nanotube and graphene nanosheet/high density polyethylene composites with a segregated network structure, Carbon 49 (4) (2011) 1094–1100.

[159]. Martin-Gallego M, Bernal M, Hernandez M, Verdejo R, López–Manchado MA, Comparison of filler percolation and mechanical properties in graphene and carbon nanotubes filled epoxy nanocomposites, Eur. Polym. J 49 (6) (2013) 1347–1353.

[160]. Gupta P, Agrawal A, Murali K, Varshney R, Beniwal S, Manhas S, Roy P, Lahiri D, Differential neural cell adhesion and neurite outgrowth on carbon nanotube and graphene reinforced polymeric scaffolds, Mater. Sci. Eng. C 97 (2019) 539–551.

[161]. Li J, Wong PS, Kim JK, Hybrid nanocomposites containing carbon nanotubes and graphite nanoplatelets, Mater. Sci. Eng. A 483 (2008) 660–663.

[162]. Kumar S, Sun L, Caceres S, Li B, Wood W, Perugini A, Maguire R, Zhong W, Dynamic synergy of graphitic nanoplatelets and multi-walled carbon nanotubes in polyetherimide nanocomposites, Nanotechnol. 21 (10) (2010) 105702.

[163]. Chen M, Zhang L, Duan S, Jing S, Jiang H, Li C, Highly stretchable conductors integrated with a conductive carbon nanotube/graphene network and 3D porous poly (dimethylsiloxane), Adv. Funct. Mater 24 (47) (2014) 7548–7556.

[164]. Kharaziha M, Shin SR, Nikkhah M, Topkaya SN, Masoumi N, Annabi N, Dokmeci MR, Khademhosseini A, Tough and flexible CNT–polymeric hybrid scaffolds for engineering cardiac constructs, Biomaterials 35 (26) (2014) 7346–7354. [PubMed: 24927679]

[165]. Mombini S, Mohammadnejad J, Bakhshandeh B, Narmani A, Nourmohammadi J, Vahdat S, Zirak S, Chitosan-PVA-CNT nanofibers as electrically conductive scaffolds for cardiovascular tissue engineering, Int. J. Biol. Macromol 140 (2019) 278–287. [PubMed: 31400428]

[166]. Zhao G, Zhang X, Li B, Huang G, Xu F, Zhang X, Solvent-free fabrication of carbon nanotube/silk fibroin electrospun matrices for enhancing cardiomyocyte functionalities, ACS Biomater. Sci. Eng 6 (3) (2020) 1630–1640. [PubMed: 33455382]

[167]. Wu Y, Wang L, Guo B, Ma PX, Interwoven aligned conductive nanofiber yarn/hydrogel composite scaffolds for engineered 3D cardiac anisotropy, ACS Nano 11 (6) (2017) 5646–5659. [PubMed: 28590127]

[168]. Zhao G, Qing H, Huang G, Genin GM, Lu TJ, Luo Z, Xu F, Zhang X, Reduced graphene oxide functionalized nanofibrous silk fibroin matrices for engineering excitable tissues, NPG Asia Mater. 10 (10) (2018) 982–994.

[169]. Stone H, Lin S, Mequanint K, Preparation and characterization of electrospun rGO-poly(ester amide) conductive scaffolds, Mater. Sci. Eng. C Mater. Biol. Appl 98 (2019) 324–332. [PubMed: 30813034]

[170]. Talebi A, Labbaf S, Karimzadeh F, Masaeli E, Nasr Esfahani MH, Electroconductive graphene-containing polymeric patch: a promising platform for future cardiac repair, ACS Biomater. Sci. Eng 6 (7) (2020) 4214–4224. [PubMed: 33463338]

[171]. Wang L, Wu Y, Hu T, Guo B, Ma PX, Electrospun conductive nanofibrous scaffolds for engineering cardiac tissue and 3D bioactuators, Acta Biomater. 59 (2017) 68–81. [PubMed: 28663141]

[172]. Guo B, Ma PX, Conducting polymers for tissue engineering, Biomacromol. 19 (6) (2018) 1764–1782.

[173]. Nezakati T, Seifalian A, Tan A, Seifalian AM, Conductive polymers: opportunities and challenges in biomedical applications, Chem. Rev 118 (14) (2018) 6766–6843. [PubMed: 29969244]

[174]. Kayser LV, Lipomi DJ, Stretchable conductive polymers and composites based on PEDOT and PEDOT: PSS, Adv. Mater 31 (10) (2019) 1806133.

[175]. Saberi A, Jabbari F, Zarrintaj P, Saeb MR, Mozafari M, Electrically conductive materials: opportunities and challenges in tissue engineering, Biomolecules 9 (9) (2019) 448.

[176]. Memic A, Alhadrami HA, Hussain MA, Aldhahri M, Al Nowaiser F, Al–Hazmi F, Oklu R, Khademhosseini A, Hydrogels 2.0: improved properties with nanomaterial composites for biomedical applications, Biomed. Mater 11 (1) (2015) 014104. [PubMed: 26694229]

[177]. Memic A, Colombani T, Eggermont LJ, Rezaeeyazdi M, Steingold J, Rogers ZJ, Navare KJ, Mohammed HS, Bencherif SA, Latest advances in cryogel technology for biomedical applications, Adv. Ther 2 (4) (2019) 1800114.

[178]. Rogers ZJ, Zeevi MP, Koppes R, Bencherif SA, Electroconductive hydrogels for tissue engineering: current status and future perspectives, Bioelectricity 2 (3) (2020) 279–292. [PubMed: 34476358]

[179]. Li MY, Bidez P, Guterman-Tretter E, Guo Y, MacDiarmid AG, Lelkes PI, Yuan XB, Yuan XY, Sheng J, Li H, Electroactive and nanostructured polymers as scaffold materials for neuronal and cardiac tissue engineering, Chin. J. Polym. Sci 25 (04) (2007) 331–339.

[180]. Baei P, Hosseini M, Baharvand H, Pahlavan S, Electrically conductive materials for *in vitro* cardiac microtissue engineering, J. Biomed. Mater. Res. Part A 108 (5) (2020) 1203–1213.

[181]. Kai D, Prabhakaran MP, Jin G, Ramakrishna S, Polypyrrole-contained electrospun conductive nanofibrous membranes for cardiac tissue engineering, J. Biomed. Mater. Res. Part A 99 (3) (2011) 376–385.

[182]. Balint R, Cassidy NJ, Cartmell SH, Conductive polymers: towards a smart biomaterial for tissue engineering, Acta Biomater. 10 (6) (2014) 2341–2353. [PubMed: 24556448]

[183]. Bhadra S, Khastgir D, Singha NK, Lee JH, Progress in preparation, processing and applications of polyaniline, Prog. Polym. Sci 34 (8) (2009) 783–810.

[184]. Qazi TH, Rai R, Boccaccini AR, Tissue engineering of electrically responsive tissues using polyaniline based polymers: a review, Biomaterials 35 (33) (2014) 9068–9086. [PubMed: 25112936]

[185]. Li M, Guo Y, Wei Y, MacDiarmid AG, Lelkes PI, Electrospinning polyaniline-contained gelatin nanofibers for tissue engineering applications, Biomaterials 27 (13) (2006) 2705–2715. [PubMed: 16352335]

[186]. Bidez PR, Li S, MacDiarmid AG, Venancio EC, Wei Y, Lelkes PI, Polyaniline, an electroactive polymer, supports adhesion and proliferation of cardiac myoblasts, J. Biomater. Sci. Polym. Ed 17 (1–2) (2006) 199–212. [PubMed: 16411609]

[187]. Borriello A, Guarino V, Schiavo L, Alvarez-Perez M, Ambrosio L, Optimizing PANi doped electroactive substrates as patches for the regeneration of cardiac muscle, J. Mater. Sci. Mater. Med 22 (4) (2011) 1053–1062. [PubMed: 21373812]

[188]. Baheiraei N, Yeganeh H, Ai J, Gharibi R, Ebrahimi-Barough S, Azami M, Vahdat S, Baharvand H, Preparation of a porous conductive scaffold from aniline pentamer-modified polyurethane/PCL blend for cardiac tissue engineering, J. Biomed. Mater. Res. Part A 103 (10) (2015) 3179–3187.

[189]. Hsiao CW, Bai MY, Chang Y, Chung MF, Lee TY, Wu CT, Maiti B, Liao ZX, Li RK, Sung HW, Electrical coupling of isolated cardiomyocyte clusters grown on aligned conductive nanofibrous meshes for their synchronized beating, Biomaterials 34 (4) (2013) 1063–1072. [PubMed: 23164424]

[190]. Hu T, Wu Y, Zhao X, Wang L, Bi L, Ma PX, Guo B, Micropatterned, electroactive, and biodegradable poly (glycerol sebacate)-aniline trimer elastomer for cardiac tissue engineering, Chem. Eng. J 366 (2019) 208–222.

[191]. Qazi TH, Rai R, Dippold D, Roether JE, Schubert DW, Rosellini E, Barbani N, Boccaccini AR, Development and characterization of novel electrically conductive PANI–PGS composites for cardiac tissue engineering applications, Acta Biomater. 10 (6) (2014) 2434–2445. [PubMed: 24561709]

[192]. Bertuoli PT, Ordoño J, Armelin E, Pérez-Amodio S, Baldissera AF, Ferreira CA, Puiggalí J, Engel E, Del Valle LJ, Alemán C, Electrospun conducting and biocompatible uniaxial and Core–Shell fibers having poly (lactic acid), poly (ethylene glycol), and polyaniline for cardiac tissue engineering, ACS Omega 4 (2) (2019) 3660–3672. [PubMed: 31459579]

[193]. Guimard NK, Gomez N, Schmidt CE, Conducting polymers in biomedical engineering, Prog. Polym. Sci 32 (8–9) (2007) 876–921.

[194]. Epstein A, Ginder J, Zuo F, Woo HS, Tanner D, Richter A, Angelopoulos M, Huang WS, MacDiarmid A, Insulator-to-metal transition in polyaniline: effect of protonation in emeraldine, Synth. Metals 21 (1–3) (1987) 63–70.

[195]. Huang ZB, Yin GF, Liao XM, Gu JW, Conducting polypyrrole in tissue engineering applications, Front. Mater. Sci 8 (1) (2014) 39–45.

[196]. Shi G, Zhang Z, Rouabhia M, The regulation of cell functions electrically using biodegradable polypyrrole–polylactide conductors, Biomaterials 29 (28) (2008) 3792–3798. [PubMed: 18602689]

[197]. Garner B, Georgevich A, Hodgson A, Liu L, Wallace G, Polypyrrole–heparin composites as stimulus-responsive substrates for endothelial cell growth, J. Biomed. Mater. Res 44 (2) (1999) 121–129. [PubMed: 10397912]

[198]. Ateh D, Navsaria H, Vadgama P, Polypyrrole-based conducting polymers and interactions with biological tissues, J. R. Soc. Interface 3 (11) (2006) 741–752. [PubMed: 17015302]

[199]. Gomez N, Schmidt CE, Nerve growth factor-immobilized polypyrrole: Bioactive electrically conducting polymer for enhanced neurite extension, J. Biomed. Mater. Res. Part A 81 (1) (2007) 135–149.

[200]. Cui Z, Ni NC, Wu J, Du GQ, He S, Yau TM, Weisel RD, Sung HW, Li RK, Polypyrrole-chitosan conductive biomaterial synchronizes cardiomyocyte contraction and improves myocardial electrical impulse propagation, Theranostics 8 (10) (2018) 2752. [PubMed: 29774073]

[201]. Zanjanizadeh Ezazi N, Ajdary R, Correia A, Mäkilä E, Salonen J, Kemell M, Hirvonen J, Rojas OJ, Ruskoaho HJ, Santos HA, Fabrication and characterization of drug-loaded conductive poly (glycerol sebacate)/nanoparticle-based composite patch for myocardial infarction applications, ACS Appl. Mater. Interfaces 12 (6) (2020) 6899–6909. [PubMed: 31967771]

[202]. Mihardja SS, Sievers RE, Lee RJ, The effect of polypyrrole on arteriogenesis in an acute rat infarct model, Biomaterials 29 (31) (2008) 4205–4210. [PubMed: 18678406]

[203]. Zarei M, Samimi A, Khorram M, Abdi MM, Golestaneh SI, Fabrication and characterization of conductive polypyrrole/chitosan/collagen electrospun nanofiber scaffold for tissue engineering application, Int. J. Biol. Macromol 168 (2021) 175–186. [PubMed: 33309657]

[204]. Spearman BS, Hodge AJ, Porter JL, Hardy JG, Davis ZD, Xu T, Zhang X, Schmidt CE, Hamilton MC, Lipke EA, Conductive interpenetrating networks of polypyrrole and polycaprolactone encourage electrophysiological development of cardiac cells, Acta Biomater. 28 (2015) 109–120. [PubMed: 26407651]

[205]. Ma C, Jiang L, Wang Y, Gang F, Xu N, Li T, Liu Z, Chi Y, Wang X, Zhao L, 3D printing of conductive tissue engineering scaffolds containing polypyrrole nanoparticles with different morphologies and concentrations, Materials 12 (15) (2019) 2491.

[206]. Ajdary R, Ezazi NZ, Correia A, Kemell M, Huan S, Ruskoaho HJ, Hirvonen J, Santos HA, Rojas OJ, Multifunctional 3D-printed patches for long-term drug release therapies after myocardial infarction, Adv. Funct. Mater 30 (34) (2020) 2003440.

[207]. Tsui JH, Ostrovsky-Snider NA, Yama DM, Donohue JD, Choi JS, Cha-vanachat R, Larson JD, Murphy AR, Kim DH, Conductive silk–polypyrrole composite scaffolds with bioinspired nanotopographic cues for cardiac tissue engineering, J. Mater. Chem. B 6 (44) (2018) 7185–7196. [PubMed: 31448124]

[208]. Abedi A, Hasanzadeh M, Tayebi L, Conductive nanofibrous chitosan/PEDOT: PSS tissue engineering scaffolds, Mater. Chem. Phys 237 (2019) 121882.

[209]. Yang B, Yao F, Ye L, Hao T, Zhang Y, Zhang L, Dong D, Fang W, Wang Y, Zhang X, A conductive PEDOT/alginate porous scaffold as a platform to modulate the biological behaviors of brown adipose-derived stem cells, Biomater. Sci 8 (11) (2020) 3173–3185. [PubMed: 32367084]

[210]. Roshanbinfar K, Vogt L, Greber B, Diecke S, Boccaccini AR, Scheibel T, Engel FB, Electroconductive biohybrid hydrogel for enhanced maturation and beating properties of engineered cardiac tissues, Adv. Funct. Mater 28 (42) (2018) 1803951.

[211]. Stejskal J, Conducting polymer hydrogels, Chem. Pap 71 (2) (2017) 269–291.

[212]. Mawad D, Mansfield C, Lauto A, Perbellini F, Nelson GW, Tonkin J, Bello SO, Carrad DJ, Micolich AP, Mahat MM, A conducting polymer with enhanced electronic stability applied in cardiac models, Sci. Adv 2 (11) (2016) e1601007. [PubMed: 28138526]

[213]. Landa N, Miller L, Feinberg MS, Holbova R, Shachar M, Freeman I, Cohen S, Leor J, Clinical perspective, Circulation 117 (11) (2008) 1388–1396. [PubMed: 18316487]

[214]. Hernandez MJ, Christman KL, Designing acellular injectable biomaterial therapeutics for treating myocardial infarction and peripheral artery disease, JACC Basic Trans. Sci 2 (2) (2017) 212–226.

[215]. Fujimoto KL, Ma Z, Nelson DM, Hashizume R, Guan J, Tobita K, Wagner WR, Synthesis, characterization and therapeutic efficacy of a biodegradable, thermoresponsive hydrogel designed for application in chronic infarcted myocardium, Biomaterials 30 (26) (2009) 4357–4368. [PubMed: 19487021]

[216]. Wang T, Wu DQ, Jiang XJ, Zhang XZ, Li XY, Zhang JF, Zheng ZB, Zhuo R, Jiang H, Huang C, Novel thermosensitive hydrogel injection inhibits post-infarct ventricle remodelling, Eur. J. Heart Fail 11 (1) (2009) 14–19. [PubMed: 19147452]

[217]. Pal A, Smith CI, Palade J, Nagaraju S, Alarcon-Benedetto BA, Kilbourne J, Rawls A, Wilson-Rawls J, Vernon BL, Nikkhah M, Poly (N-isopropylacry-lamide)-based dual-crosslinking biohybrid injectable hydrogels for vascularization, Acta Biomater. 107 (2020) 138–151. [PubMed: 32126310]

[218]. He S, Wu J, Li SH, Wang L, Sun Y, Xie J, Ramnath D, Weisel RD, Yau TM, Sung HW, Li RK, The conductive function of biopolymer corrects myocardial scar conduction blockage and

resynchronizes contraction to prevent heart failure, Biomaterials 258 (2020) 120285. [PubMed: 32781327]

[219]. Mihic A, Cui Z, Wu J, Vlacic G, Miyagi Y, Li SH, Lu S, Sung HW, Weisel RD, Li RK, A conductive polymer hydrogel supports cell electrical signaling and improves cardiac function after implantation into myocardial infarct, Circulation 132 (8) (2015) 772–784. [PubMed: 26304669]

[220]. Ulery BD, Nair LS, Laurencin CT, Biomedical applications of biodegradable polymers, J. Polym. Sci. Part B Polym. Phys 49 (12) (2011) 832–864.

[221]. Wang L, Jiang J, Hua W, Darabi A, Song X, Song C, Zhong W, Xing MM, Qiu X, Mussel-inspired conductive cryogel as cardiac tissue patch to repair myocardial infarction by migration of conductive nanoparticles, Adv. Funct. Mater 26 (24) (2016) 4293–4305.

[222]. Zhou J, Chen J, Sun H, Qiu X, Mou Y, Liu Z, Zhao Y, Li X, Han Y, Duan C, Tang R, Wang C, Zhong W, Liu J, Luo Y, Mengqiu Xing M, Wang C, Engineering the heart: evaluation of conductive nanomaterials for improving implant integration and cardiac function, Sci. Rep 4 (2014) 3733. [PubMed: 24429673]

[223]. Wu T, Cui C, Huang Y, Liu Y, Fan C, Han X, Yang Y, Xu Z, Liu B, Fan G, Liu W, Coadministration of an adhesive conductive hydrogel patch and an injectable hydrogel to treat myocardial infarction, ACS Appl. Mater. Interfaces 12 (2) (2020) 2039–2048. [PubMed: 31859471]

[224]. Song C, Zhang X, Wang L, Wen F, Xu K, Xiong W, Li C, Li B, Wang Q, Xing MMQ, Qiu X, An Injectable conductive three-dimensional elastic network by tangled surgical-suture spring for heart repair, ACS Nano 13 (12) (2019) 14122–14137. [PubMed: 31774656]

[225]. Hosoyama K, Ahumada M, McTiernan CD, Davis DR, Variola F, Ruel M, Liang W, Suuronen EJ, Alarcon EI, Nanoengineered electroconductive collagen-based cardiac patch for infarcted myocardium repair, ACS Appl. Mater. Interfaces 10 (51) (2018) 44668–44677. [PubMed: 30508481]

[226]. Zhang C, Hsieh MH, Wu SY, Li SH, Wu J, Liu SM, Wei HJ, Weisel RD, Sung HW, Li RK, A self-doping conductive polymer hydrogel that can restore electrical impulse propagation at myocardial infarct to prevent cardiac arrhythmia and preserve ventricular function, Biomaterials 231 (2020) 119672. [PubMed: 31841751]

[227]. Chen S, Hsieh MH, Li SH, Wu J, Weisel RD, Chang Y, Sung HW, Li RK, A conductive cell-delivery construct as a bioengineered patch that can improve electrical propagation and synchronize cardiomyocyte contraction for heart repair, J. Control Release 320 (2020) 73–82. [PubMed: 31958479]

[228]. Paul A, Hasan A, Kindi HA, Gaharwar AK, Rao VT, Nikkhah M, Shin SR, Krafft D, Dokmeci MR, Shum-Tim D, Khademhosseini A, Injectable graphene oxide/hydrogel-based angiogenic gene delivery system for vasculogenesis and cardiac repair, ACS Nano 8 (8) (2014) 8050–8062. [PubMed: 24988275]

[229]. Zhou J, Yang X, Liu W, Wang C, Shen Y, Zhang F, Zhu H, Sun H, Chen J, Lam J, Injectable OPF/graphene oxide hydrogels provide mechanical support and enhance cell electrical signaling after implantation into myocardial infarct, Theranostics 8 (12) (2018) 3317. [PubMed: 29930732]

[230]. Bao R, Tan B, Liang S, Zhang N, Wang W, Liu W, A pi-pi conjugation-containing soft and conductive injectable polymer hydrogel highly efficiently re-builds cardiac function after myocardial infarction, Biomaterials 122 (2017) 63–71. [PubMed: 28107665]

[231]. Wang W, Tan B, Chen J, Bao R, Zhang X, Liang S, Shang Y, Liang W, Cui Y, Fan G, Jia H, Liu W, An injectable conductive hydrogel encapsulating plasmid DNA-eNOs and ADSCs for treating myocardial infarction, Biomaterials 160 (2018) 69–81. [PubMed: 29396380]

[232]. Fu X, Khalil H, Kanisicak O, Boyer JG, Vagnozzi RJ, Maliken BD, Sargent MA, Prasad V, Valiente-Alandi I, Blaxall BC, Molkentin JD, Specialized fibroblast differentiated states underlie scar formation in the infarcted mouse heart, J. Clin. Invest 128 (5) (2018) 2127–2143. [PubMed: 29664017]

[233]. Liau B, Zhang D, Bursac N, Functional cardiac tissue engineering, Regen. Med 7 (2) (2012) 187–206. [PubMed: 22397609]

[234]. Liang S, Zhang Y, Wang H, Xu Z, Chen J, Bao R, Tan B, Cui Y, Fan G, Wang W, Wang W, Liu W, Paintable and rapidly bondable conductive hydrogels as therapeutic cardiac patches, Adv. Mater 30 (23) (2018) e1704235. [PubMed: 29687502]

[235]. Malki M, Fleischer S, Shapira A, Dvir T, Gold nanorod-based engineered cardiac patch for suture-free engraftment by near IR, Nano Lett. 18 (7) (2018) 4069–4073. [PubMed: 29406721]

[236]. Ribeiro J, Caseiro AR, Pereira T, Armada-da-Silva PA, Pires I, Prada J, Amorim I, Leal Reis I, Amado S, Santos JD, Evaluation of PVA biodegradable electric conductive membranes for nerve regeneration in axonotmesis injuries: the rat sciatic nerve animal model, J. Biomed. Mater. Res. Part A 105 (5) (2017) 1267–1280.

[237]. Guex AG, Puetzer JL, Armgarth A, Littmann E, Stavrinidou E, Giannelis EP, Malliaras GG, Stevens MM, Highly porous scaffolds of PEDOT: PSS for bone tissue engineering, Acta Biomater. 62 (2017) 91–101. [PubMed: 28865991]

[238]. Mousavi A, Vahdat S, Baheiraei N, Razavi M, Norahan MH, Baharvand H, Multifunctional conductive biomaterials as promising platforms for cardiac tissue engineering, ACS Biomater. Sci. Eng 7 (1) (2020) 55–82. [PubMed: 33320525]

[239]. Wang P, Wang X, Wang L, Hou X, Liu W, Chen C, Interaction of gold nanoparticles with proteins and cells, Sci. Technol. Adv. Mater 16 (3) (2015) 034610. [PubMed: 27877797]

[240]. Song X, Wang X, Zhang J, Shen S, Yin W, Ye G, Wang L, Hou H, Qiu X, A tunable self-healing ionic hydrogel with microscopic homogeneous conductivity as a cardiac patch for myocardial infarction repair, Biomaterials 273 (2021) 120811. [PubMed: 33882404]

[241]. Goenka S, Sant V, Sant S, Graphene-based nanomaterials for drug delivery and tissue engineering, J. Controll. Release 173 (2014) 75–88.

[242]. Bianco A, Graphene: safe or toxic? The two faces of the medal, Angew. Chem. Int. Ed 52 (19) (2013) 4986–4997.

[243]. Kaur G, Adhikari R, Cass P, Bown M, Gunatillake P, Electrically conductive polymers and composites for biomedical applications, RSC Adv. 5 (47) (2015) 37553–37567.

[244]. He Y, Hou H, Wang S, Lin R, Wang L, Yu L, Qiu X, From waste of marine culture to natural patch in cardiac tissue engineering, Bioact. Mater 6 (7) (2021) 2000–2010. [PubMed: 33426372]

[245]. Shi H, Xue T, Yang Y, Jiang C, Huang S, Yang Q, Lei D, You Z, Jin T, Wu F, Microneedle-mediated gene delivery for the treatment of ischemic myocardial disease, Sci. Adv 6 (25) (2020) eaaz3621. [PubMed: 32596444]

[246]. Christman KL, Biomaterials for tissue repair, Sci. 363 (6425) (2019) 340–341.

[247]. Esmaeili H, Li C, Fu X, Jung JP, Engineering extracellular matrix proteins to enhance cardiac regeneration after myocardial infarction, Front. Bioeng. Biotechnol 8 (2020) 611936. [PubMed: 33553118]

[248]. Bassat E, Mutlak YE, Genzelinakh A, Shadrin IY, Umansky KB, Yifa O, Kain D, Rajchman D, Leach J, Bassat DR, The extracellular matrix protein agrin promotes heart regeneration in mice, Nature 547 (7662) (2017) 179–184. [PubMed: 28581497]

[249]. Jung JP, Hu D, Domian IJ, Ogle BM, An integrated statistical model for enhanced murine cardiomyocyte differentiation via optimized engagement of 3D extracellular matrices, Sci. Rep 5 (1) (2015) 1–13.

Statement of significance

Myocardial infarction (MI) is still the primary cause of death worldwide. Over the past decade, electroconductive biomaterials have increasingly been applied in the field of cardiac tissue engineering. This review article provides the readers with the leading advances in the *in vitro* applications of electroconductive biomaterials for cTE along with an in-depth discussion of injectable/transplantable electroconductive biomaterials and their delivery methods for *in vivo* MI treatment. The article also discusses the knowledge gaps in the field and offers possible novel avenues for improved cardiac tissue engineering.

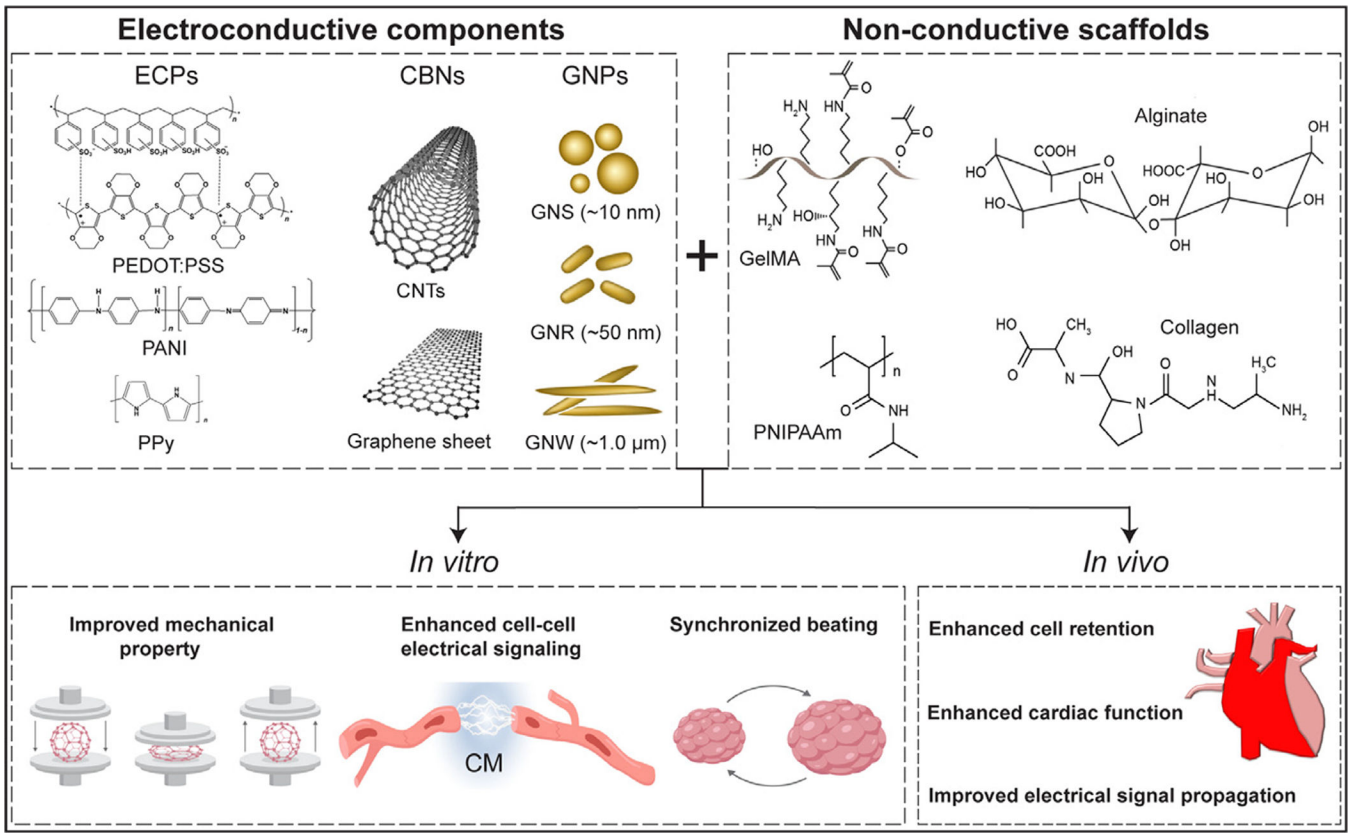

Fig. 1.

The common conductive materials and non-conductive scaffolds used in cTE. The electroconductive components endow electrical features to the non-conductive scaffold generating cardiac tissues mimicking the native microenvironment. Abbreviations: ECPs (electroconductive polymers), PEDOT:PSS (poly(3,4-ethylenedioxythiophene) polystyrene sulfonate), PANI (polyaniline), PPy (polypyrrole), CNTs (carbon nanotubes), GNPs (gold nanoparticles), CBNs (carbon-based nanomaterials), GNS (gold nanosphere), GNR (gold nanorod), GNW (gold nanowire), GelMA (gelatin methacrylate), PNIPAAm (poly(N-isoproylacrylaminde)), CM (cardiomyocyte).

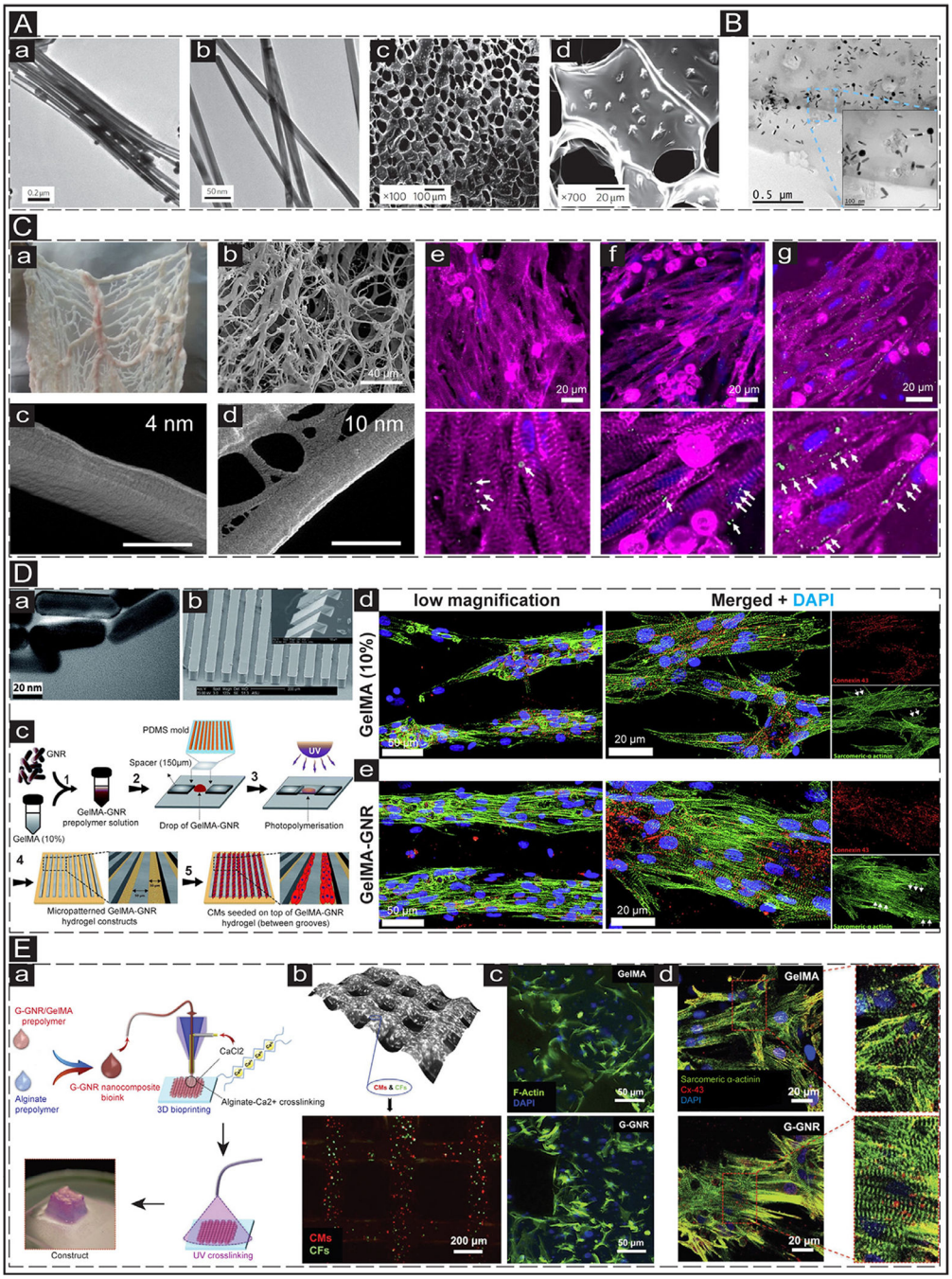

Fig. 2.

In vitro application of GNPs in cTE. (**A**) Alginate scaffolds embedded with GNWs. **a**&**b**: Transmission electron microscopy (TEM) images of the synthesized GNWs. **c**&**d**: SEM images showing the distribution of the GNWs (1 mg/mL) within the porous structure of the alginate scaffold. Adapted with permission from [115]. Copyright © 2011, Nature. (**B**) The TEM image shows the distribution of GNRs (1.5 mg/mL) within the GelMA hydrogel. Adapted with permission from [119]. Copyright © 2016, Elsevier. (**C**) The decellularized omentum tissue deposited with GNSs. **a**: native omentum tissue before decellularization.

b: decellularized omentum tissue. **c**&**d**: SEM images showing the scaffolds deposited with 4 and 10 nm GNSs. The scale bar is 500 nm. **e**-**g**: Cardiac-specific marker (Cx-43 (green) and sarcomeric α-actinin (pink)) expression of CMs cultured on pristine (e), 4 nm (f), and 10 nm (g) decellularized omentum scaffolds. The bottom panels show the magnified images. The scale bar is 20 μm. Adapted with permission from [120]. Copyright © 2014, American Chemical Society. (**D**) NRVMs cultured on micropatterned GelMA-GNR scaffold. **a**: TEM images of the synthesized GNRs. The scale bar is 20 nm. **b**: SEM image exhibits the patterned PDMS grooves. The scale bar is 200 μm. **c**: Schematic illustrating the fabrication process of patterned microgrooves. **d**&**e**: IF images show the expression of cardiac-specific markers (sarcomeric α-actinin (green) and Cx-43 (red)) in the CMs cultured on the micropatterned pristine GelMA (10%) (d) and GelMA-GNRs (e) scaffolds at day 7. Adapted with permission from [124]. Copyright © 2017, Royal Society of Chemistry. (**E**) 3D bioprinted scaffolds generated from GelMA-GNR scaffold. **a**: Schematic illustrating the 3D bioprinting process using the GNR-GelMA bioink. **b**: Brightfield image showing the distribution of cells in the bioprinted constructs using GNR nanocomposite (0.1 mg/mL G-GNR, 2% alginate, 7% GelMA) (top panel); distribution of CMs (red) and cardiac fibroblasts (CFs) (green) in the bioprinted constructs (bottom panel). **c**: IF images showing F-actin (green) expression in the cardiac cells within the bioprinted GelMA/alginate and GNR nanocomposite constructs at day 5. **d**: IF images show the expression of cardiac-specific markers (Cx-43 (red) and sarcomeric α-actinin (green)) in the CMs cultured on the printed pristine GelMA (10%) (top panel) and GelMA-GNRs (bottom panel) scaffolds at day 14. Adapted with permission from [126]. Copyright © 2017, John Wiley and Sons.

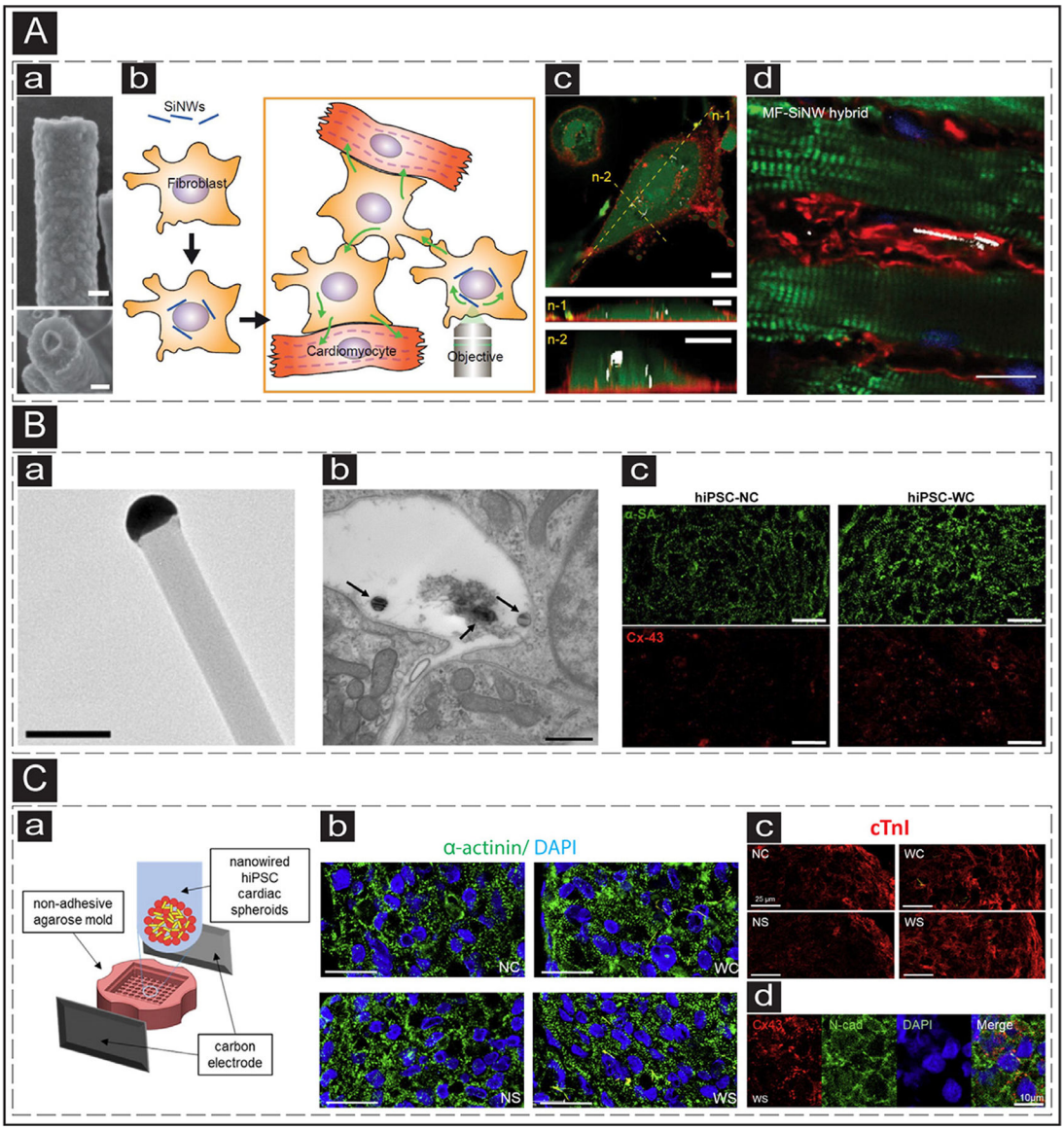

Fig. 3.

The use of Silicon-based electroconductive nanoparticles in cTE. (**A**) **a**: SEM image of a SiNW. **b**: Schematic representation of utilization of optoelectric SiNWs for indirect stimulation of CMs. **c**: Confocal image of a myofibroblast with internalized SiNW. n-1 and n-2 represent cross-sectional slices (green: cytoplasm, red: cellular membrane). The scale bars are 10 μm. **d**: IHC image showing injected MF-SiNWs adjacent to viable CMs. Adapted with permission from [132]. Copyright © PNAS. (**B**) **a**: TEM image of an eSiNW. The scale bar is 0.2 μm. **b**: TEM image of a cardiac spheroid with eSiNWs (black arrows) in the intercellular space. The scale bar is 500nm. **c**: IF staining of microtissues without (left) and with (right) eSiNWs, showing increased expression of sarcomeric α-actinin (green) and Cx-43 (red). The scale bars are 20 μm. Adapted with permission from [133]. Copyright © American Chemical Society. (**C**) **a**: Schematic representation of the formation of electrically stimulated cardiac spheroids with addition of eSiNWs. **b**: sarcomeric organization of hiPSC-

CMs in cardiac spheroids (upper left: no eSiNWs, no electrical stimulation; upper right: eSiNWs, no electrical stimulation; lower left: no eSiNWs, electrical stimulation; lower right: eSiNWs and electrical stimulation) (green: sarcomeric α-actinin, blue: nuclei). The scale bars are 25 μm. **c**: IF image showing enhanced expression of cTnI (red) of the hiPSC-CMs in the spheroids with electrical stimulation and eSiNWs (lower right). The scale bars are 25 μm. **d**: Expression of cell-cell junction proteins of the hiPSC-CMs in the spheroids with electrical stimulation and eSiNWs (red: Cx-43, green: N-cadherin, blue: nuclei). The scale bar is 10 μm. Adapted with permission from [134]. Copyright © American Chemical Society.

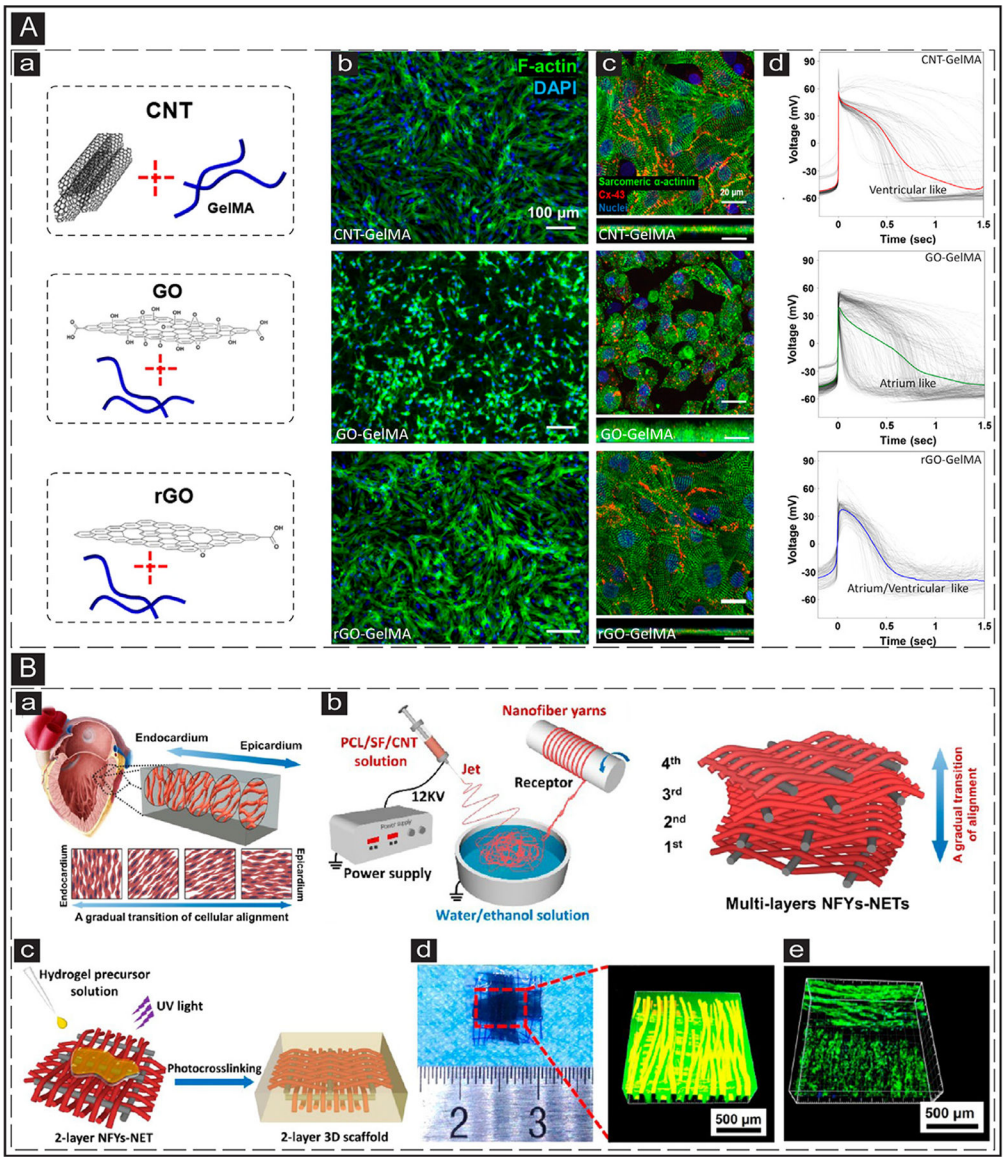

Fig. 4.

In vitro application of CBNs in cTE. (**A**) **a**: Schematic representation of GelMA-based hydrogels incorporated with CNT, GO, and rGO. **b**: IF images showing CMs morphology after five days of culture on CNT-, GO-, and rGO-GelMA biohybrids. F-Actin and cell nuclei are visualized in green and blue, respectively. **c**: Cardiac biomarker expressed by CMs after five days of culture on CNT-, GO-, and rGO-GelMA biohybrids. Sarcomeric α-actinin and Cx-43 are visualized in green and red, respectively. **d**: Action potential measured from CMs matured for five days on CNT-, GO-, and rGO-GelMA biohybrids. Adapted with permission from [143]. Copyright © 2019, American Chemical Society. (**B**) **a**: Schematic illustration of cardiac muscle fibrils and their gradual alignment transition within the myocardium. **b**: A scheme showing typical wet-dry electrospinning employed to manufacture CNT-incorporated silk-based mats with a gradual transition of orientation between interwoven layers. **c**: Schematic representation of the process used to embed the

2-layer electrospun network in GelMA hydrogel and its crosslinking. **d**: A gross photo of the fabricated 2-layer 3D scaffold and its confocal imaging showing the orthogonally woven nanofibers inside the hydrogel construct. **e**: The confocal image showing cell alignment on the perpendicular layers of nanofibers within the hydrogel network. Adapted with permission from [167]. Copyright © 2019, American Chemical Society.

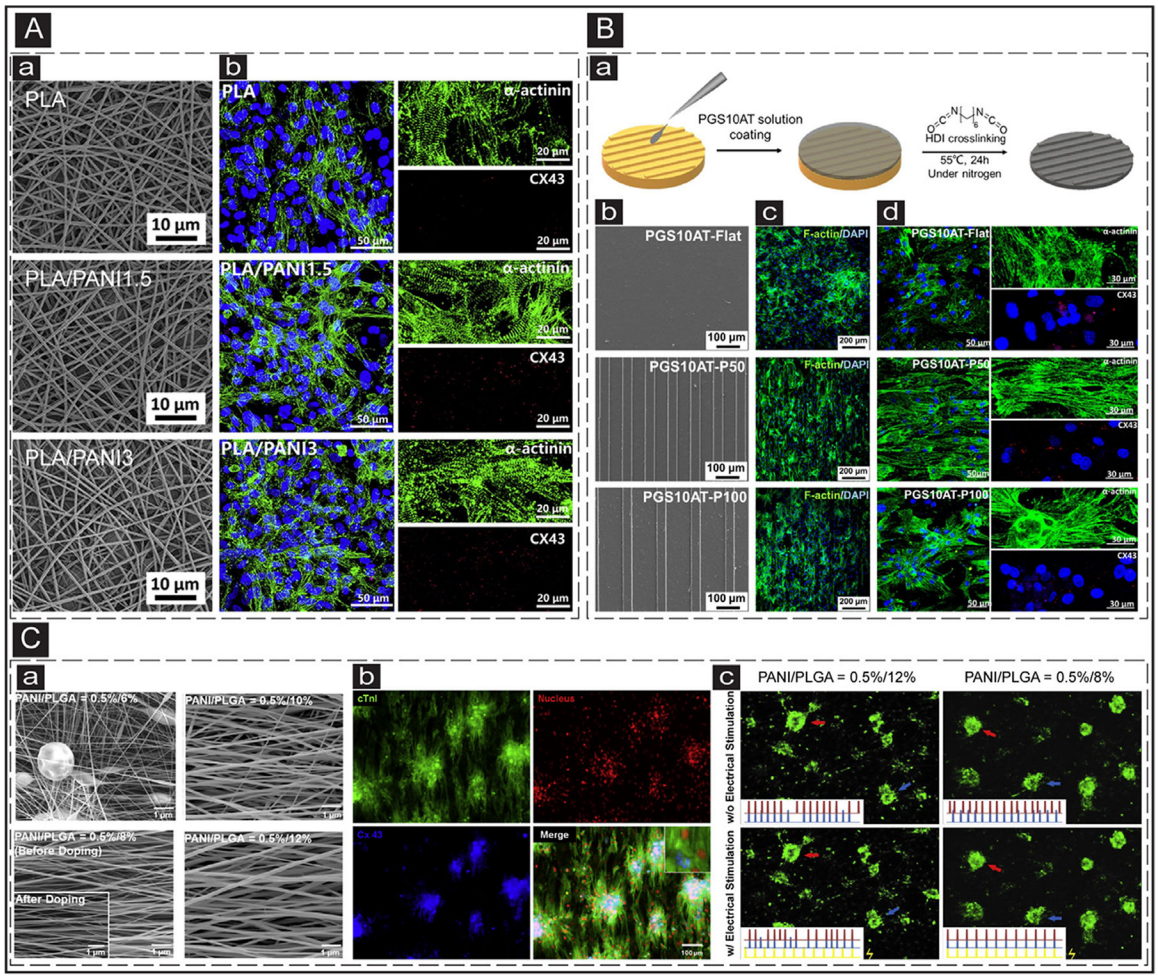

Fig. 5.

ECPs application in cTE. (**A**) Electrospun nanofibrous constructs for cTE. **a**: SEM images of the electrospun PLA scaffolds with different PANI contents. **b**: IF images show the cardiac-specific markers (Cx-43 (red) and sarcomeric α-actinin (green)) expression in the CMs cultured on the electrospun scaffolds with various PANI contents. Adapted with permission from [171]. Copyright © 2017, Elsevier. (**B**) Micropatterned electroconductive PGS-aniline scaffolds for cTE. **a**: Schematic illustrating the process of PGS10AT-6H micropatterns. **b**: SEM images of the patterned PGS10AT films. **c**: IF images show F-actin (green) expression in the CMs cultured on patterned scaffolds after two days. **d**: IF images of the expression of cardiac-specific markers (α-actinin (green) and Cx-43 (red)) in the CMs cultured on the scaffolds after eight days. Adapted with permission from [190]. Copyright © 2019, Elsevier. (**C**) Electrical coupling of separated CMs cultured on electrospun conductive PANI/PLGA nanofibrous scaffolds. **a**: SEM images of the electrospun PANI/PLGA scaffolds with various ratios of PANI/PLGA (w/v). **b**: IF images of the expression of cardiac-specific markers (cTnI (green) and Cx-43 (blue)) in the CMs cultured on the doped fibrous scaffolds. **c**: Beating frequencies of the CMs clusters cultured on the low (PNAI/PLGA = 0.5/12%) and high (PNAI/PLGA = 0.5/8%) conductive scaffolds prior and after electrical stimulation.

The red, blue, and yellow signals correspond to the red arrow, blue arrow, and stimulated electrical signals. Adapted with permission from [189]. Copyright © 2013, Elsevier.

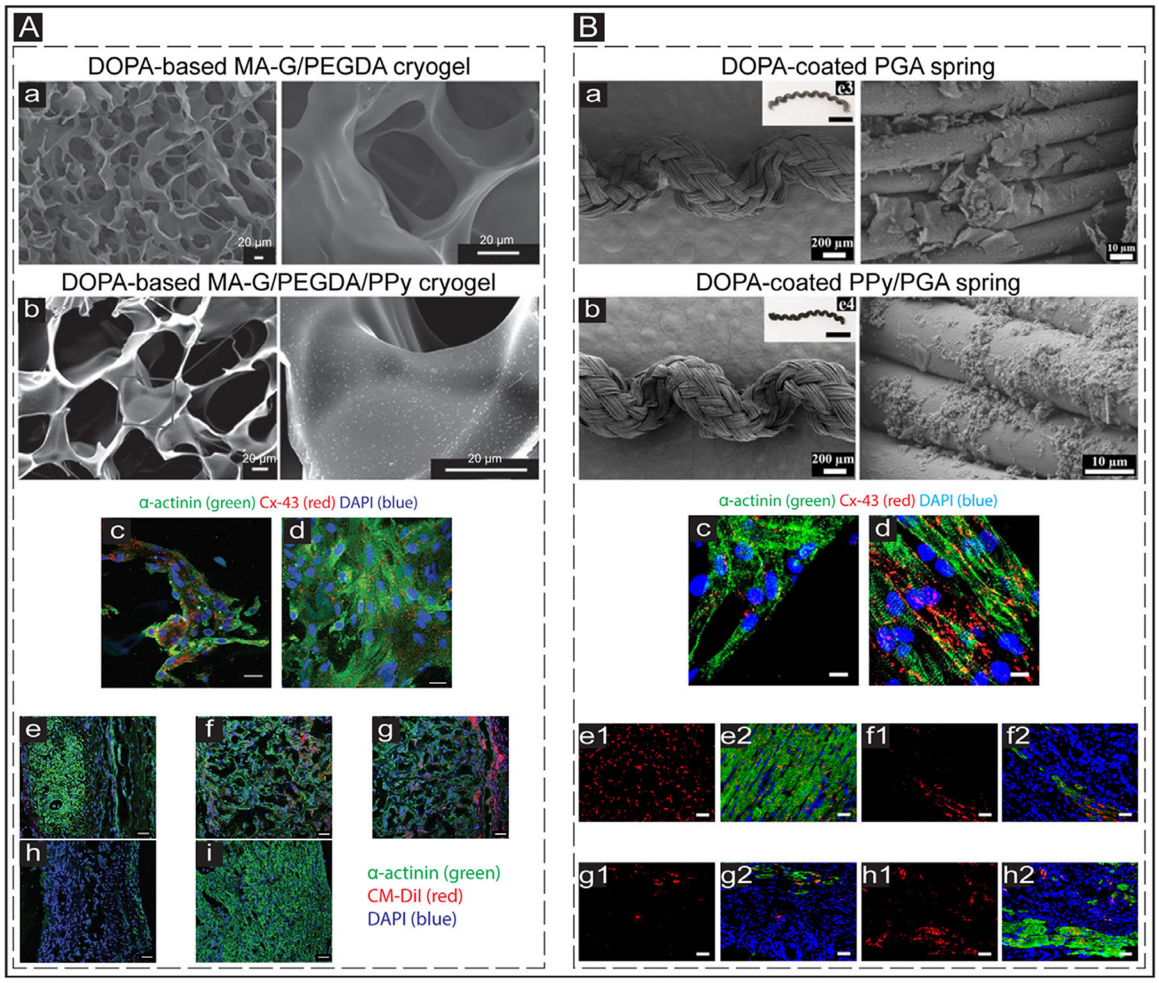

Fig. 6.

In vivo application of conductive biomaterials for cardiac regeneration after MI. (**A**) **a&b**: Scanning electron microscopy (SEM) images showing the structure of conductive and non-conductive cryogels. The PPy concentration in the conductive cyogel (b) was 2 mg/mL. The scale bar is 20 μm. **c&d**: IF images exhibit the expressed cardiac-specific markers (α-actinin (green) and Cx-43 (red)) in the CMs cultured on DOPA-based MA-G/PEGDA (c) and DOPA-based MA-G/PEGDA/PPy (d) at day 8 *in vitro*. The scale bar is 50 μm. **e-i**: IF images showing the expression of CM-DiI labeled (red) CMs and α-actinin (green) in the infarcted hearts treated with DOPA-based MA-G/PEGDA/PPy patch. e: Infarcted myocardium; f: Middle part of the transplanted conductive patch; g: External region of the transplanted patch; h: Infarct zone of the myocardium of the treated animals; i: Healthy tissue of the myocardium (control). The scale bar is 50 μm. Adapted with permission from [221]. Copyright © 2016, John Wiley and Sons. (**B**) **a&b**: SEM images showing the structure of non-conductive (DOPA-coated PGA) and conductive (DOPA-coated PPy/PGA) biosprings. **c&d**: Expressed cardiac-specific markers (α-actinin (green) and Cx-43 (red)) in the CMs cultured on DOPA-coated PGA (c) and DOPA-coated PPy/PGA (d) springs at day 7 *in vitro*. The scale bar is 10 μm. **e-h**: Images showing the cardiac-specific markers (α-actinin (green) and Cx-43 (red)) expression in the hearts of treated animals. e1&e2:

Sham group; f1&f2: Infarcted group; g1&g2: Non-conductive spring (DOPA-coated PGA) group; h1&h2: Conductive spring (DOPA-coated PPy/PGA) group. The scale bar is 50 μm. Adapted with permission from [224]. Copyright © 2019, American Chemical Society.

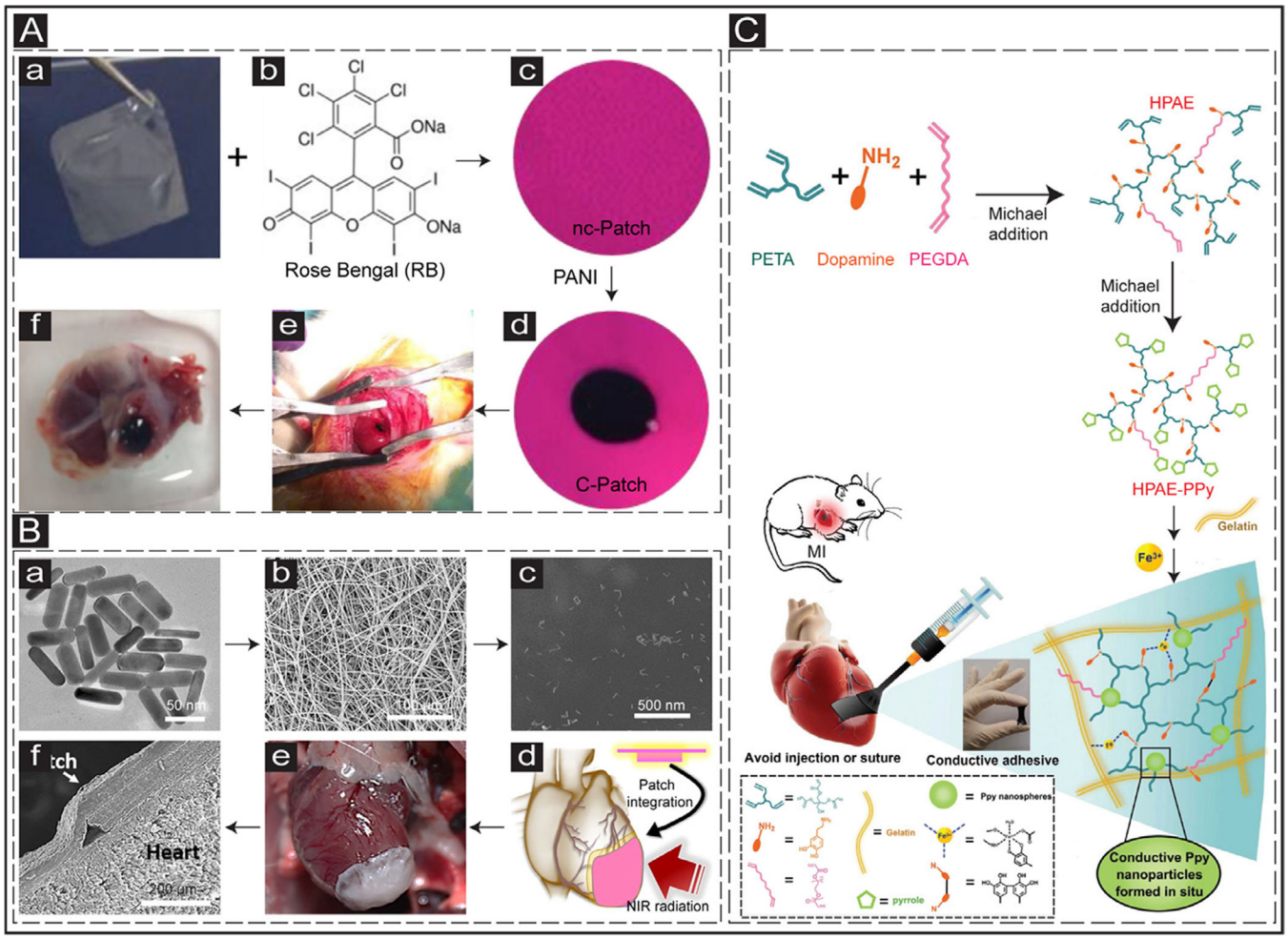

Fig. 7.

Suture-free methods for the delivery of cardiac patches *in vivo*. (**A**) **a**: CHI film. **b&c**: Rose Bengal is added to the CHI film making a non-conductive photoactivated patch (nc-Patch). **d**: PANI is immobilized into the nc-Patch, making a conductive patch (c-Patch). **e**: Transplantation of the c-Patch into the rat heart through photoadhesion. **f**: Explanted heart after two weeks *in vivo*. Adapted with permission from [212]. Copyright © 2016, American Association for the Advancement of Science. (**B**) Suture-free GNR-based cardiac patch. **a**: Synthesized GNRs. **b**: SEM image of electrospun albumin scaffolds. **c**: SEM image of incorporated GNRs into the fibrous scaffolds. **d**: Scheme illustrating the transplantation of cardiac patch into the beating heart by NIR radiation. **e**: Integration of the cardiac patch with the rat heart. **f**: SEM image of the integrated patch and the heart tissue. Adapted with permission from [235]. Copyright © 2018, American Chemical Society. (**C**) Schematic showing the development of a paintable conductive cardiac patch. Adapted with permission from [234]. Copyright © 2018, John Wiley and Sons.

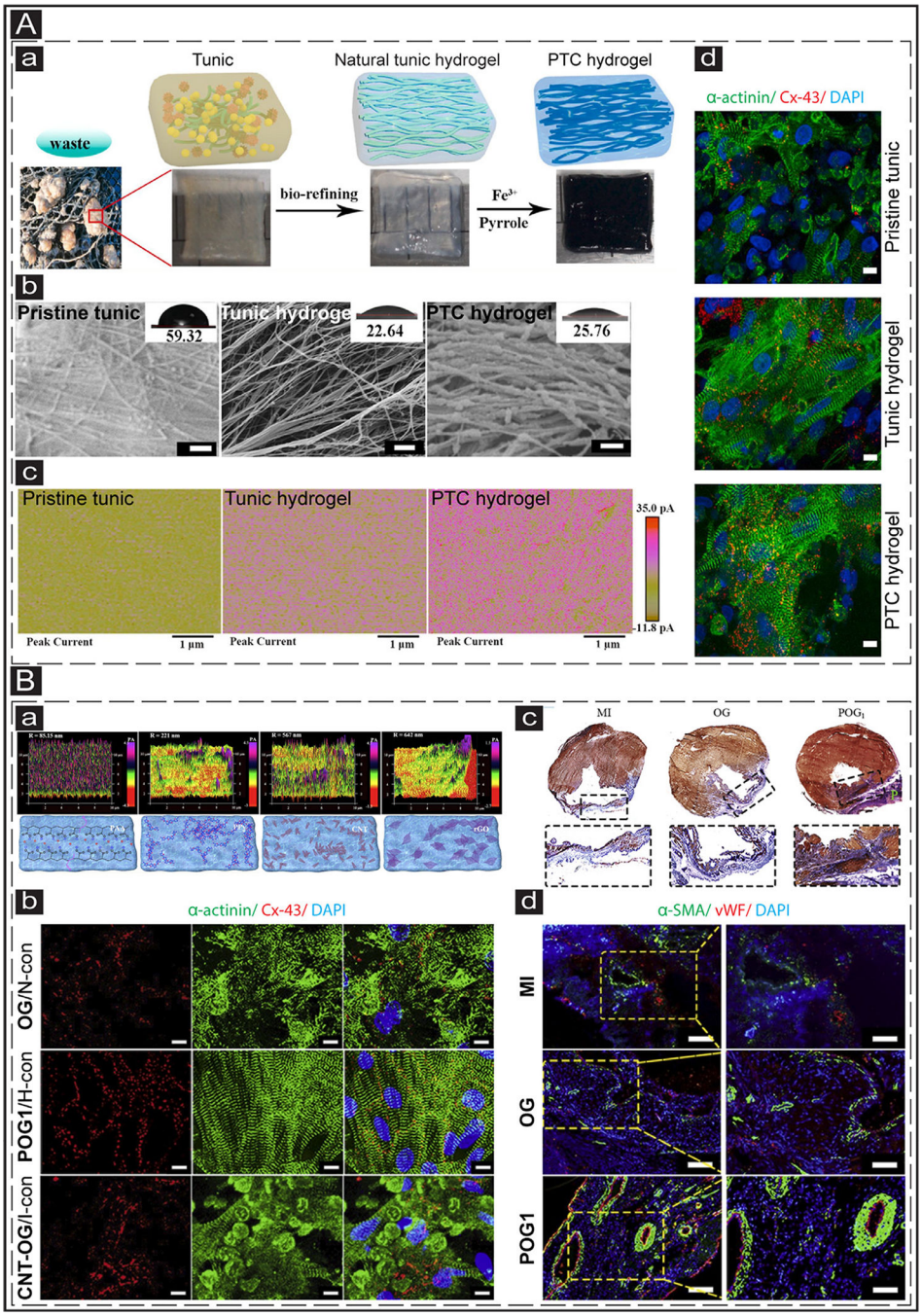

Fig. 8.

Application of animal-based self-conductive and ionic conductive hydrogels in cTE. (**A**) Fabrication of a functional cardiac patch derived from natural self-conductive tunic cellulose. **a**: Schematic representing the procedure for preparation of pristine tunic, tunic hydrogel, and PTC hydrogel. **b**: SEM images showing the structure of the pristine tunic, tunic hydrogel, and PTC hydrogel. The insets show the contact angles of each surface. The scale bar is 200 nm. **c**: Images show the current distribution within the pristine tunic, tunic hydrogel, and PTC hydrogel measured by e-AFM. **d**: IF images show the cardiac-specific

markers (sarcomeric α-actinin (green) and Cx-43 (red)) expression in the NRVMs cultured on the pristine tunic, tunic hydrogel, and PTC hydrogel. The scale bar is 20 μm. Adapted with permission from [244]. Copyright © 2021, Elsevier. (**B**) Cardiac patches derived from the ionic conductive hydrogel. **a**: The conductivity measurement of different hydrogels including POG1, PPy-OG, CNT-OG, and rOG-OG (Upper pictures), using AFM. The lower pictures show the schematic of each hydrogel. **b**: IF images show the cardiac-specific markers (sarcomeric α-actinin (green) and Cx-43 (red)) expression in the NRVMs cultured on OG/N-con, POG1/H-con, and CNT-OG/I-con for 7 days. The scale bar is 10 μm. N-con: Non-conductive; H-con: High-conductivity; I-con: Inhomogeneous-conductive. **c**: Masson's trichrome staining images of the various hydrogel groups (MI, OG, and POG1) after 4 weeks. **d**: α-SMA (green) and vWF (red) staining with infarct areas at 4 weeks post-transplantation of cardiac patches. The scale bar for column 1 and column 2 is 50 μm and 25 μm, respectively. Adapted with permission from [240]. Copyright © 2021, Elsevier.

Table 1

Summary of the *in vivo* use of conductive biomaterials for cardiac regeneration after MI.

Type of conductive biomaterial	Cell-laden/ cell-free	Method for delivery	Animal injury model	Results	Year/Ref.
PPy blended with alginate	Cell-free	Intramyocardial injection	Rat model of ischemia-reperfusion MI	Induced arteriogenesis; increased migration of myofibroblasts to the infarct zone; no inflammation; no significant change in scar size.	2008/ [202]
GelMA with nanocomplexes of GO	Cell-free	Intramyocardial injection	Rat model acute MI via left coronary artery ligation	Enhanced myocardial capillary density; reduced scar size; improved cardiac function.	2014/ [228]
PNIAPAAm hydrogel with SWCNTs	Cell-laden: BASCs	Intramyocardial injection	Rat model of MI via left coronary artery ligation	Enhanced retention of seeded cells; differentiation of BASCs to CMs.	2014/[85]
SWNTs loaded into gelatin hydrogel	Cell laden: NRVCs	Suturing on epicardial surface	Rat model of MI via left coronary artery ligation	Formation of aligned cell bundles; enhanced expression of N-cadherin and Cx-43; host vasculature invasion to the transplanted constructs at 1 week post implantation; Accumulation of $CD68^{+}$ macrophages in the scar areas.	2014/ [222]
Grafting pyrrole to CHI generating a semi-conductive hydrogel (PPy:CHI)	Cell-free	Intramyocardial Injection	Rat model of MI via left coronary artery ligation	Improved cardiac contractile function at 8 weeks after injection; no significant difference in scar size.	2015/ [219]
Distribution of PPy nanoparticles into GelMA, and poly(ethylene glycol) diacrylate in the form of cryogel using dopamine crosslinker (DOPA-based MA-G/ PEGDA/PPy cryogel)	Cell laden: NRVMs	Sutured onto the epicardium	Rat model of MI via left coronary artery ligation	Enhanced cardiac function; reduced scar size; improved electric conduction across the infarcted region.	2016/ [221]
PANI doped with phytic acid on a CHI surface	Cell-free	Patch transplantation onto the epicardium via photoadhesion	Rat model of MI via left coronary artery ligation	No proarrhythmogenic induction at 2 weeks post transplantation; no significant improvement in heart function; some level of neovascularization.	2016/ [212]
GO introduced to synthesized multi-armed crosslinker PEGDA700-Melamine (PEG-MEL) crosslinked with thiol modified hyaluronic acid (HA-SH) (PEG-MEL/HA-SH/GO) acute MI via left coronary artery ligation	Cell-laden: ADSCs	Intramyocardial injection	Rat model	Pronounced expression of a-SMA and Cx-43; improved heart function; thicker LV wall; reduced scar size at 4 weeks post injection.	2017/ [230]
GO introduced into oligo(poly(ethylene glycol) fumarate) (OPF) hydrogels (OPF/GO)	Cell-free	Intramyocardial injection	Rat model of MI via left coronary artery ligation	Increased expression of gap junction proteins; improved heart function; enhanced neovascularization; improved Ca^{2+} signal conduction of CMs; thicker LV wall; reduced scar size at 4 weeks post injection.	2018/ [229]
Reaction of conducting crosslinker tetraaniline-polyethylene glycol diacrylate (TA-PEG) and thiolated hyaluronic acid (HA-SH) (TA-PEG/HA-SH)	Cell-laden: ADSCs	Intramyocardial injection	Rat model acute MI via left coronary artery ligation	Improved cardiac function; pronounced expression of Cx-43 and sarcomeric a-actinin; reduced infarct size; increased vessel density.	2018/ [231]
Collagen incorporated with GNSs	Cell-free	Cardiac patch transplantation onto epicardium surface via fibrin sealant	Rat model of MI by via left coronary artery ligation	Reduced scar size; enhanced expression of Cx-43 and sarcomeric α-actinin; increased vasculogenesis within the infarcted area; no induction of ventricular tachycardia.	2018/ [225]

Type of conductive biomaterial	Cell-laden/ cell-free	Method for delivery	Animal injury model	Results	Year/Ref.
Conjugating conductive PPy onto CHI backbones	Cell-free	Intramyocardial injection	Rat model of MI by cryoablation on the lateral wall of the LV	Enhanced propagation of electrical signals across the infarcted tissue; improved cardiac function without inducing arrhythmias at 4 weeks post injection.	2018/ [200]
Hyperbranched poly(amino ester) (HPAE)-PPy/Gelatin hydrogels	Cell-free	Conductive adhesive patch painted to the surface of the heart	Rat model acute MI via left coronary artery ligation	Reduced scar size; thicker LV wall; pronounced expression of Cx-43; increased generation of new vessels within the scar tissues.	2018/ [234]
Albumin electrospun fibers and GNRs	Cell-laden: rat LV cardiac cells	Suture-free transplantation of cardiac patch by illumination with near IR laser (808 nm)	Rat model of MI via left coronary artery ligation	No reported in vivo data	2018/ [235]
Thermal plastic poly(glycolic acid) (PGA) surgical suture coated with PPy (biospring)	Cell-free	Intramyocardial injection	Rat acute model of MI via left coronary artery ligation	Increased angiogenesis; improved expression of Cx-43 and a-actinin; reduced infarct size.	2019/ [224]
Conjugated pyrrole into CHI synthesizing a poly-pyrrole-CHI (PPY-CHI) hydrogel	Cell-free	Intramyocardial injection	Rat model of MI via left coronary artery ligation	Induced angiogenesis; reduced scar size; enhanced cardiac function at 3 months post injection without inducing arrhythmias.	2020/ [218]
Self-adhesive conductive patch: dopamine-gelatin (GelDA) conjugates and dopamine-functionalized PPy (DA-PPy) Injectable hydrogel: oxidized sodium hyaluronic acid (HA-CHO) and hydrazided hyaluronic acid (HHA)	Cell-free	Codelivery of the conductive self-adhesive cardiac patch and an injectable hydrogel	Rat model of MI via left coronary artery ligation	Increased expression of Cx-43 and sarcomeric α-actinin; improved cardiac function; thicker LV wall; enhanced angiogenesis at 4 weeks post injection.	2020/ [223]
Grafting poly-3-amino-4-methoxybenzoic acid (PAMB) onto non-conductive gelatin crosslinked via carbodiimide (PAMB-G)	Cell-free	Intramyocardial injection	Rat model of MI via left coronary artery ligation	Improved cardiac function; reduced scar size; thicker LV wall; no sign of arrhythmia induction.	2020/ [226]
Gelatin-based gelfoam conjugated with poly-3-amino-4-methoxybenzoic acid (PAMB)	Cell-laden: NRVMs	Epicardial delivery of the cardiac patch	Rat model of MI via left coronary artery ligation	Improved cardiac function; improved propagation of electrical impulse; reduced arrhythmias at four weeks post transplantation.	2020/ [227]
Tunic cellulose derived natural self-conductive biomaterial with or without PPy	Cell-laden: NRVMs	Epicardial delivery of the cardiac patch	Rat model of MI via the ligation of left anterior descending	Improved cardiac function; reduced infarct size; increased LV wall thickness; induced angiogenesis; enhanced expression of Cx-43 and organized sarcomeric α-actinin; increased expression of M2 macrophages specific marker (MRC1)	2021/ [244]
Incorporation of hydrophilic ionic polymer polyacrylic acid (PAA) into the oxidized alginate (OA)/gelatin (Geln)	Cell-laden: NRVMs	Epicardial delivery of the cardiac patch	Rat model of MI via the ligation of left anterior descending	Improved cardiac function; reduced fibrosis; increased LV wall thickness; induced angiogenesis	2021/ [240]